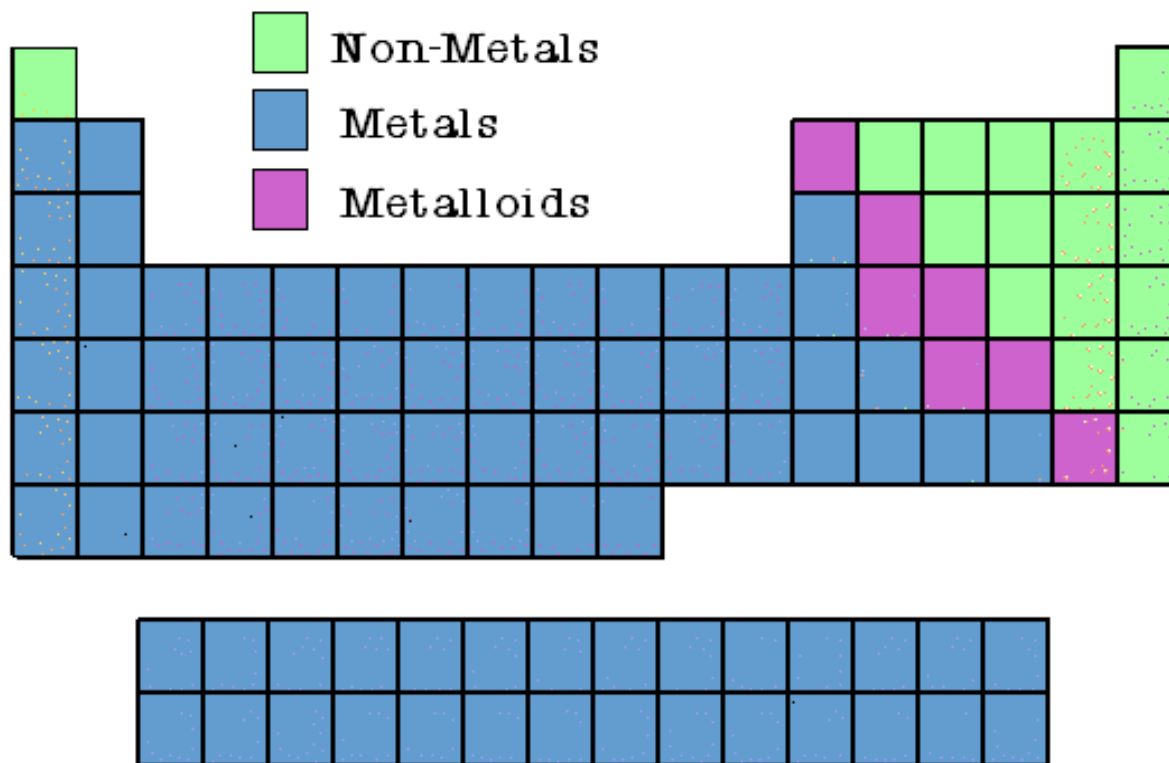


# Chapter 4 Computational design of metal systems

- **An overview on metals**
- 0-Dimensional System: magic clusters
- Growth of quantum-sized metallic films
  - One Dimensional Metal System: Metal Atom Wires
  - Two Dimensional Metal System:
    - A brief overview of quantum growth
    - From precise structural control to property optimization
- Nano Plasmonics

# Periodic Table

The elements of the periodic table can be divided into three main categories: Metals, Non-Metals, and Metalloids.



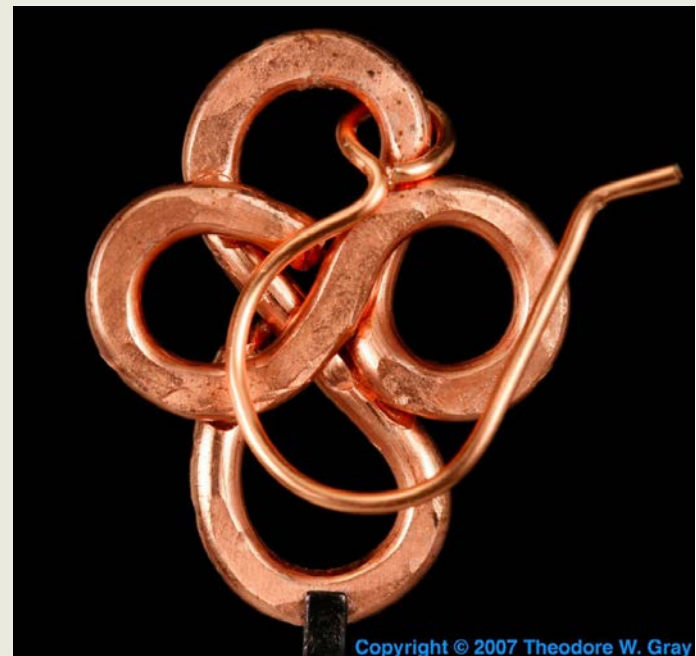
# General Properties of a Metal

- Metal is usually a **close packed structure allowing maximum sharing of valence electrons** in a non-directional bond
- High electrical conductivity, decreasing when increasing T
- Absorbs visible light (non-transparent, “shiny” due to re-emission).
- **Good alloy formation** (due to non-directional metallic bonds).
- Small cohesive energy, low melting points

# Properties of Metals

## Ductile

Metals can be drawn into wire and hammered into sheets



# Properties of Metals

## Conductors

Metals are good conductors of electricity and heat



# Properties of Metals


A chemical property of metal is its reaction with water and oxygen. This results in **corrosion** and **rust**.



# Free-electron-gas model (Drude)

- All valence electrons are completely delocalized
- The remaining positive metallic ions are immobile.
- The density of the electron gas is typically  $n \sim 10^{22}/\text{cm}^3$ , much larger than in a real gas. Nevertheless, interactions with other electrons and with ions are neglected in-between collisions
- **Sommerveld:** all electrons occupy distinct electronic states
  - The energy distribution follows the Fermi-Dirac statistics

# Electronic States of a Free Electron Gas

- The number of states depends on the volume of the system!
- The Fermi wavevector  $k_F = (3\pi^2\rho)^{1/3}$  depends on the density of conduction electrons, not on the mass. The energy does depend on mass.
- Even at  $T = 0\text{K}$  most electrons are in a state of finite energy: they are moving!
- A typical Fermi energy  $E_F = \frac{h}{2m} \left(\frac{3\rho}{8\pi}\right)^{2/3} \sim 3 \text{ eV}$  corresponds to a temperature of around  $\left(\frac{3}{0.025}\right) * 300 = 36000\text{K}$ !
- Only a minority fraction  $k_B T / E_F$  of the electrons can be thermally excited.
- Note  $N(E) = 4\pi \left(\frac{2m}{h^2}\right)^{3/2} \sqrt{E}$ ,  $\int_{E_1}^{E_2} N(E) dE =$  number of states per unit volume in a certain energy range   $E_{tot} = \frac{3}{5} N E_F$

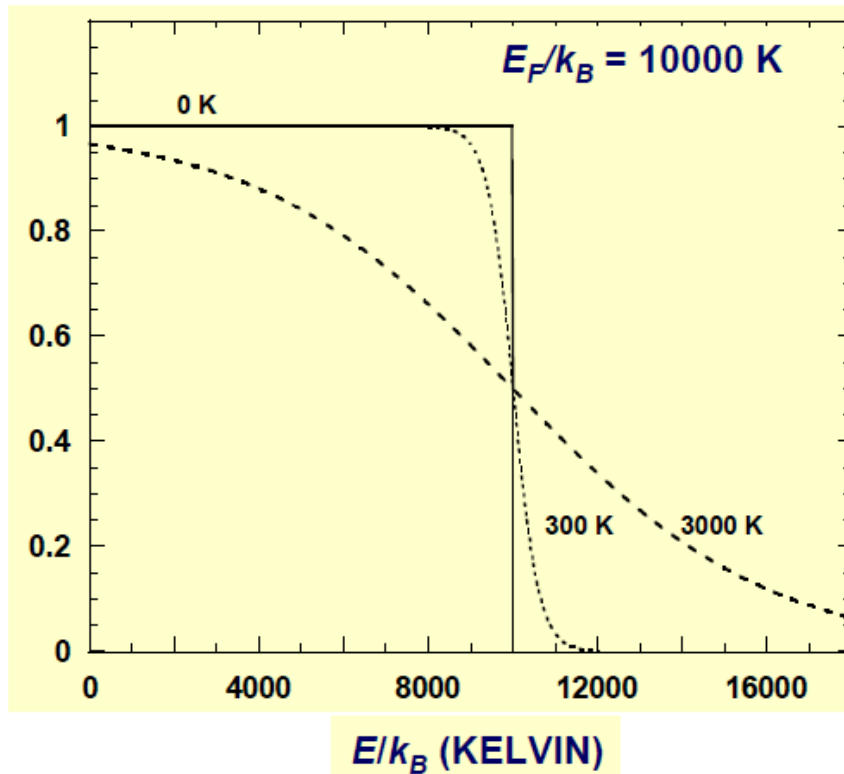


# Fermi-Dirac distribution function

For  $T > 0\text{K}$  the density of occupied states  $N(E)_{occ} = f(E) \cdot N(E)$

$$f(E) = \frac{1}{e^{\frac{E-E_F}{kT}} + 1}$$

FERMI FUNCTION  $f(E)$



$f(E)$  gives the probability that a state at a given energy  $E$  is occupied by an electron

At  $T=0\text{K}$  all states are occupied up to the  $E_F$ .

If we increase the temperature from absolute zero we SUPPLY thermal energy to electrons.

Those close to  $E_F$  move to occupy HIGHER energy states

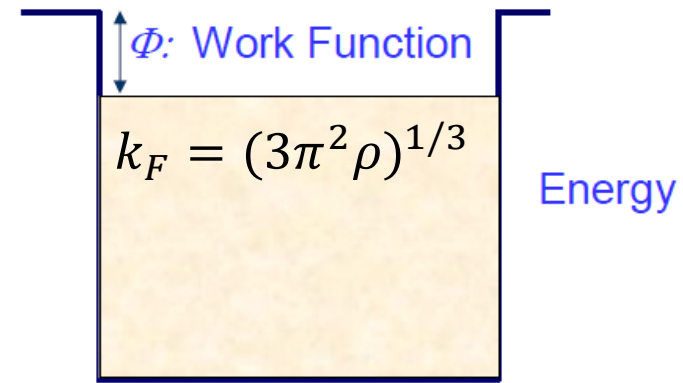
$$f(E = E_F + 3k_B T) = \frac{1}{e^3 + 1} \approx 5\%$$

# Fermi Parameters for Free Electron Metals

Fermi Energy  $E_F = \frac{\hbar^2 k_F^2}{2m}$

Fermi Velocity:  $v_F = \frac{\hbar k_F}{m}$

Fermi Temp.  $T_F = \frac{E_F}{k_B}$



Element	Electron Density, $n_e$ [ $10^{28} \text{ m}^{-3}$ ]	Fermi Energy $E_F$ [eV]	Fermi Temperature $T_F$ [ $10^4$ K]	Fermi Wavelength $\lambda_F$ [Å]	Fermi Velocity $v_F$ [ $10^6$ m/s]	Work Function $\Phi$ [eV]
Na	2.65	3.24	3.77	6.85	1.07	2.35
Cu	8.47	7.00	8.16	4.65	1.57	4.44
Ag	5.86	5.49	6.38	5.22	1.39	4.3
Au	5.90	5.53	6.42	5.22	1.40	4.3
Fe	17.0	11.1	13.0	2.67	1.98	4.31
Al	18.1	11.7	13.6	3.59	2.03	4.25
Sn	14.8	10.2	11.8	3.83	1.9	4.38

# Electronic Specific Heat

## Electronic contribution:

In a classical picture all electrons would contribute, however, the specific heat is only 1% from that expected

Only the electrons close to  $E_F$  contribute

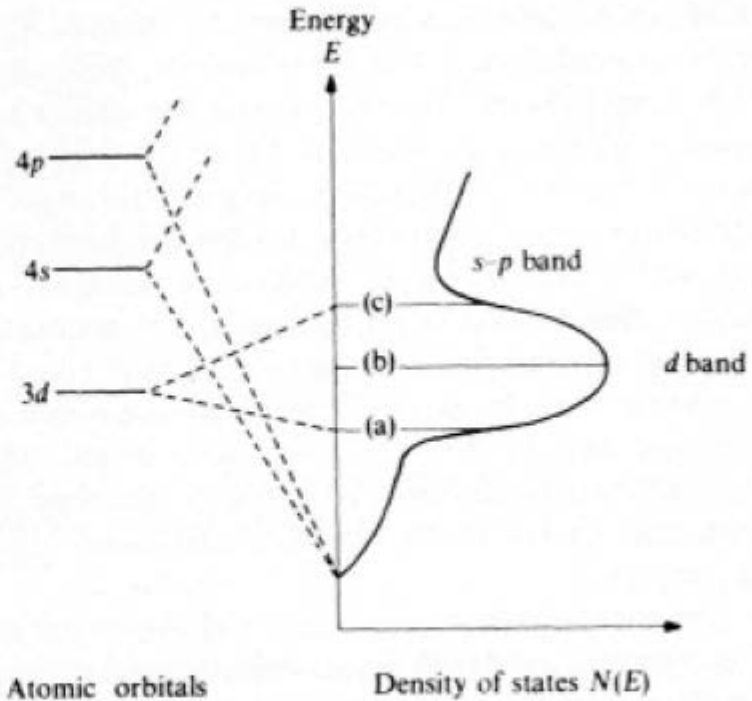
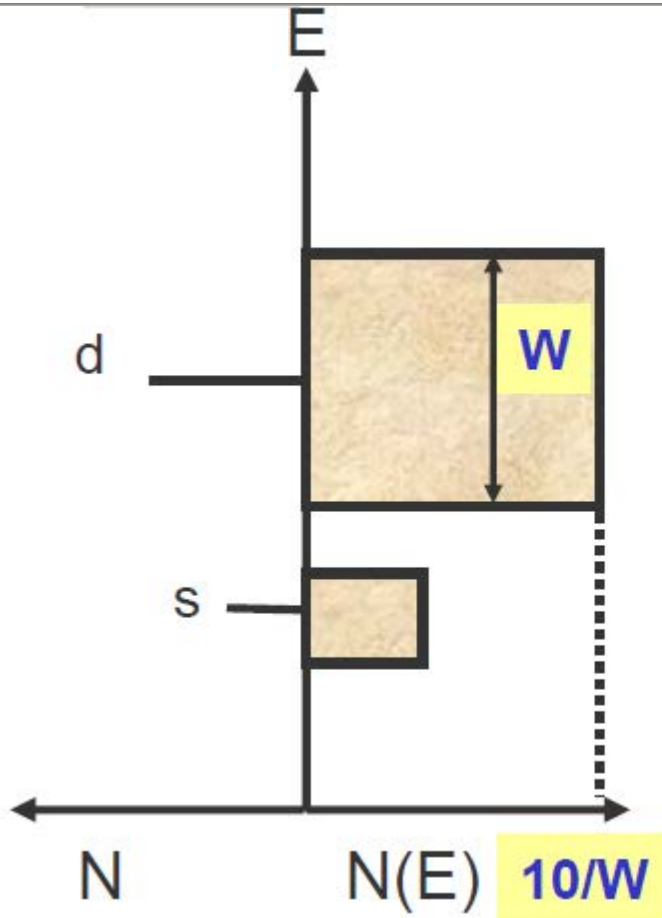
- $N$  is total number of electrons. Only a fraction  $3kT/E_F$  is excited
- $3NkT/E_F$  excited electrons
- Each has a thermal energy of the order  $kT$
- Total electronic thermal energy is  $U \cong 3N(kT)^2/E_F$
- $C_e = dU/dT \cong 6Nk^2T/E_F$

$$N = \frac{8\pi V}{3} \left( \frac{2mE_F}{h^2} \right)^{3/2}$$



$$C_e = \frac{\pi}{3} N(E_F) k^2 T$$

# Transition Metals



g. 3.13 Density of states resulting from the overlap of 3d, 4s and 4p atomic orbitals in a first-row transition metal. The Fermi level is indicated for elements: (a) early; (b) in the middle, and (c) late in the series.

$$\int_{E_1}^{E_2} N(E) dE = 10 \quad \text{free electrons/atom for } d^{10}$$

# Transition Metals

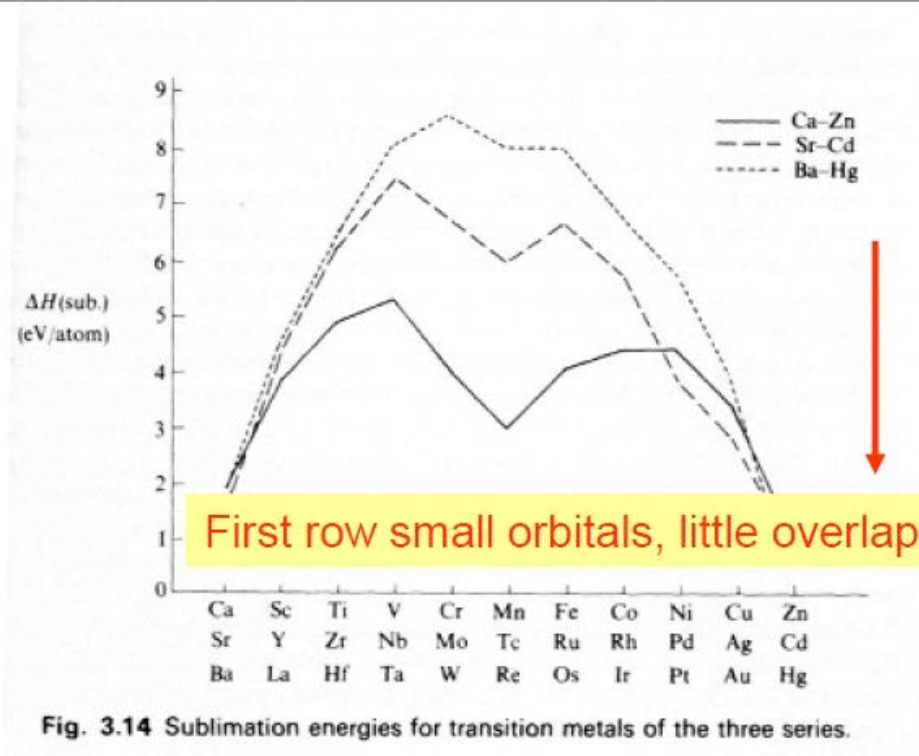
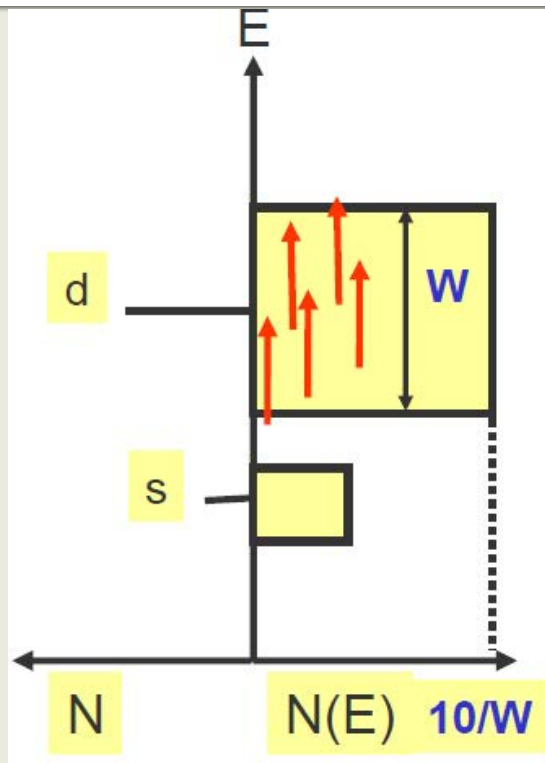
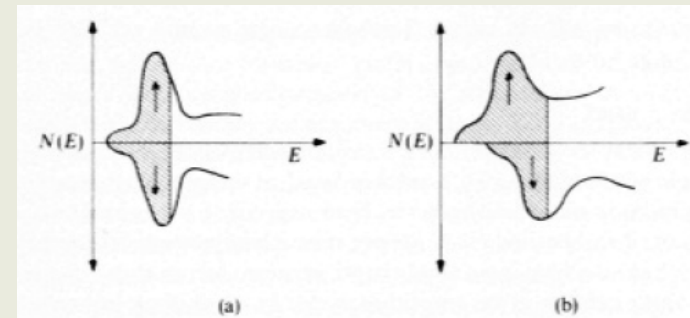


Fig. 3.14 Sublimation energies for transition metals of the three series.

- Half filling of the band energy results in a gain in energy compared to the atomic levels
- Dip in the middle due to spin alignment (Hunds rule)
- The alignment of spins reduces the electrostatic repulsion (exchange energy  $K$ ) between them.



$$K > W/5$$

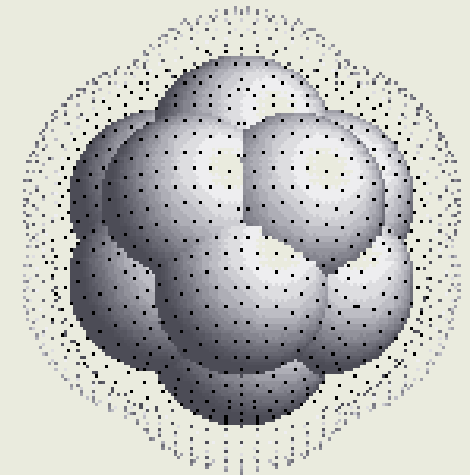
# Models of Metals

- **Jellium Model (Drude free-electron model)**
  - Uniform positive charge due to the ions, and **homogeneous electron charge** as well.
  - Focus on **electrons**.
- **Effective Medium Theory (EMT)**
  - Norskov group.
  - Focus on **ions**.
- **Embedded Atom Method (EAM)**
  - Sandia group.
  - Focus on **ions**

EMT & EAM share similar underlying principles and have comparable ranges of applicability.

# Concepts Within the Jellium Model

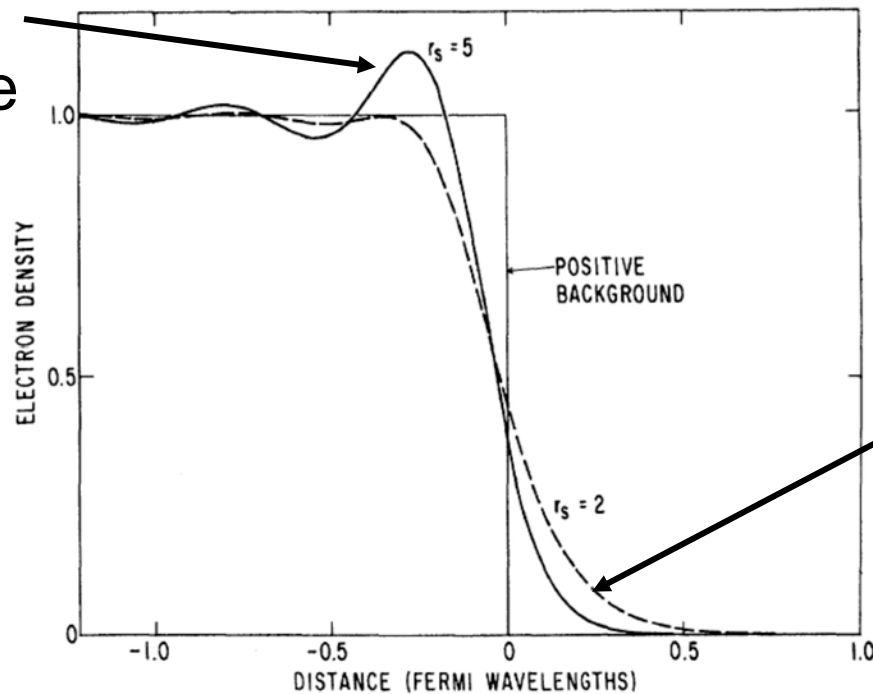
- In Bulk:
  - Electron-hole pairs
  - Plasmons
  - Many other electrical and optical properties
- At Surfaces:
  - **Work functions**
  - Image potentials
  - Charge oscillations and spilling
  - Dipolar layers
- Clusters---Magic vs. Non-magic



# Modeling Surfaces

## The jellium model

Friedel oscillations  
in the electron  
density near the  
surface



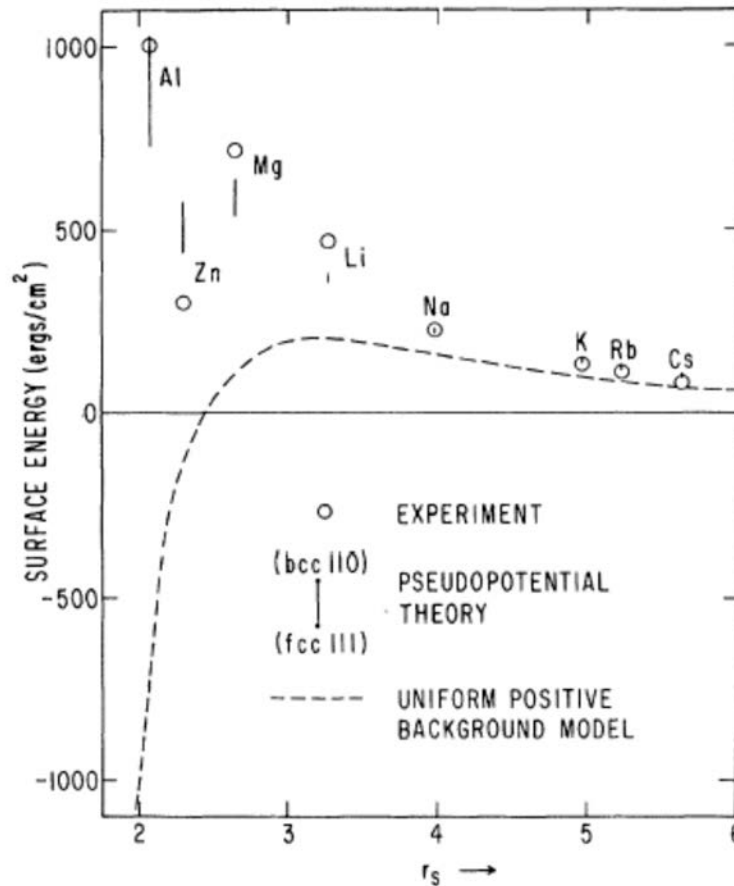
electrons spill out  
from the surface

Lang and Kohn, PRB 1,4555(1970) (the first?)



# Limitations of Jellium Model

Lang and Kohn, PRB 1,4555(1970)



Jellium model predicts that the surface energy diverges for metals with high electron density!

- An overview on metals
- **0-Dimensional System: magic clusters**
- Growth of quantum-sized metallic films
  - One Dimensional Metal System: Metal Atom Wires
  - Two Dimensional Metal System:
    - A brief overview of quantum growth
    - From precise structural control to property optimization
- Nano Plasmonics

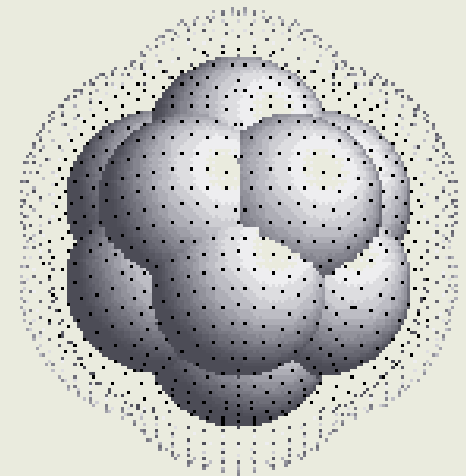
# Why Clusters?

- Clusters as Superatoms

Serving as important bridges between concepts between atoms and solids

- “Small is different”

- ✓ Chemical
- ✓ Magnetic
- ✓ Optical
- ✓ ...



# The findings of Magic number in inert gas and simple metal clusters

VOLUME 47, NUMBER 16

PHYSICAL REVIEW LETTERS

19 OCTOBER 1981

---

## Magic Numbers for Sphere Packings: Experimental Verification in Free Xenon Clusters

O. Echt, K. Sattler, and E. Recknagel

*Fakultät für Physik, Universität Konstanz, D-7750 Konstanz, West Germany*

(Received 10 April 1981; revised manuscript received 28 July 1981)

The existence of magic numbers for atomic microclusters has been found experimentally for the first time. The magic numbers  $n^*$  manifest themselves in the mass spectra of free xenon clusters, nucleated in the gas phase. The observed numbers  $n^* = 13, 55, \text{ and } 147$  coincide with the numbers of spheres required for complete-shell icosahedra. The appearance of further magic numbers (19, 25, 71, and 87) is only partially explained by previous calculations.

*Mass spectra reveal*

*Magic numbers, indicating stability and structure*

# The magic number of inert gas:

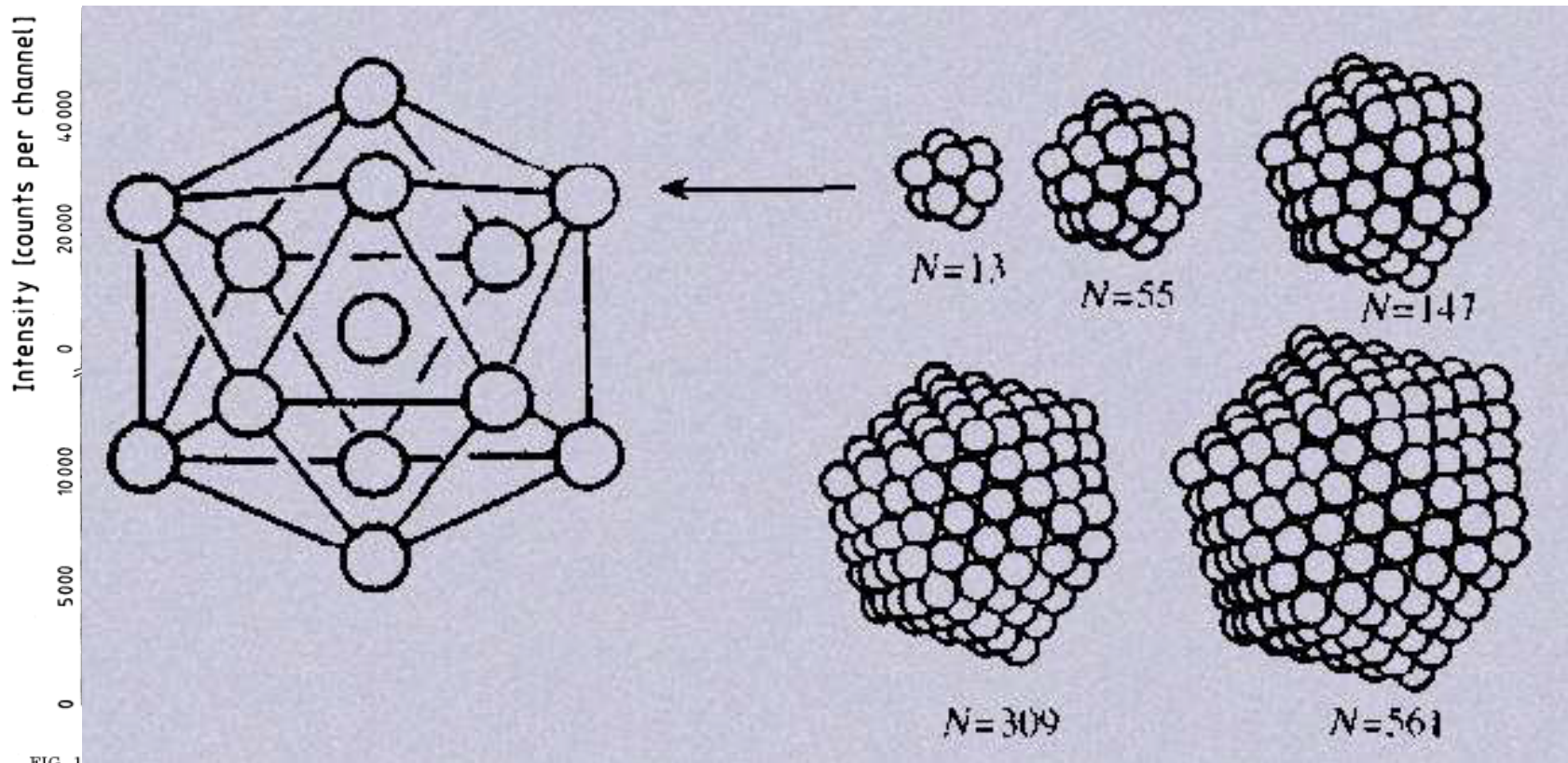


FIG. 1. for numbers with less pronounced effects. Numbers below the curve indicate predictions or distinguished sphere packings.

$$n = 1 + \sum_{l=1}^p (10l^2 + 2)$$

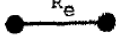
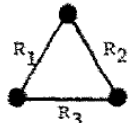
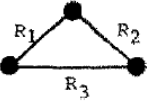
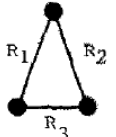
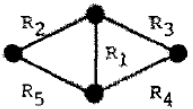
# Clusters are molecules that can be calculated using density functional theory

Surface Science 106 (1981) 280–286  
North-Holland Publishing Company

## PSEUDOPOTENTIAL SPIN-DENSITY-FUNCTIONAL CALCULATION OF THE ELECTRONIC PROPERTIES OF SMALL LITHIUM AND SODIUM CLUSTERS

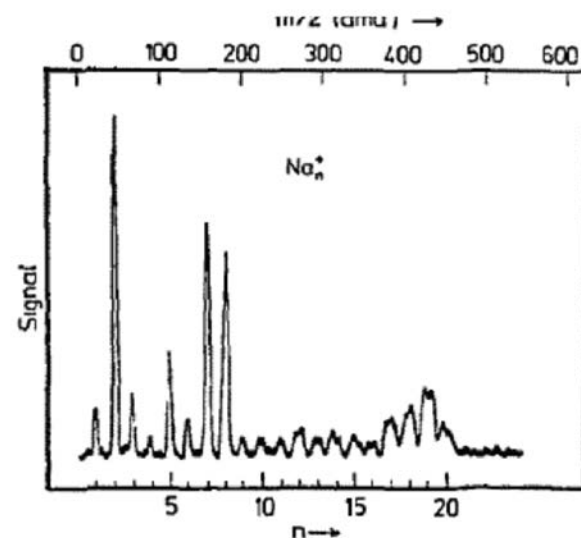
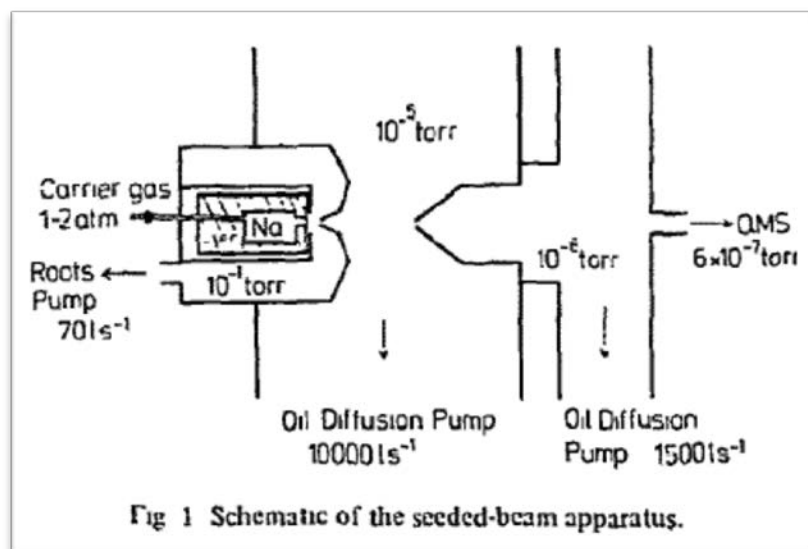
R. CAR and J.L. MARTINS

*Laboratoire de Physique Expérimentale, Ecole Polytechnique Fédérale, Lausanne, Switzerland*

Cluster	Geometry	Results
Na <sub>2</sub>		$R_e = 5.77$ (exp. [21]: 5.82; CI [24]: 5.93; AE-LD [9]: 5.74; HF-LD [18]: 5.72) BE = 0.65 (exp. [21]: 0.72; CI [24]: 0.72; AE-LD [9]: 0.65; HF-LD [18]: 0.61) $\omega_e = 163$ (exp. [21]: 159; CI [24]: 156; AE-LD [9]: 160; HF-LD [18]: 168) IP = 4.87 (exp. [21, 2]: 4.90; HF-LD [18]: 5.01)
Na <sub>3</sub> <sup>‡</sup>		$R_1 = R_2 = R_3 = 6.43$ BE = 2.14
Na <sub>3</sub> (a)		$R_1 = R_2 = 6.08$ (CI [6]: 6.25; HF-LD [18]: 6.1) $R_3 = 8.04$ (CI [6]: 7.47; HF-LD [18]: 9.1) BE = 0.86 (CI [6]: 1.14; HF-LD [18]: 0.86) IP = 4.01 (exp [2]: 3.97; HF-LD [18]: 4.25)
Na <sub>3</sub> (b)		$R_1 = R_2 = 6.81$ (CI [6]: 7.01; HF-LD [18]: 7.15) $R_3 = 5.86$ (CI [6]: 6.06; HF-LD [18]: 5.7) BE = 0.82 (CI [6]: 1.11; HF-LD [18]: 0.84) IP = 3.97 (exp. [2]: 3.97; HF-LD [18]: 4.01)
Na <sub>4</sub>		$R_1 = 5.7$ (HF-LD [18]: 5.7) $R_2 = R_3 = R_4 = R_5 = 6.1$ (HF-LD [18]: 6.64) BE = 1.92 (HF-LD [18]: 1.37) IP = 4.62 (exp. [2]: 4.27; HF-LD [18]: 3.97)

# PRODUCTION OF LARGE SODIUM CLUSTERS ( $\text{Na}_x, x \leq 65$ ) BY SEEDED BEAM EXPANSIONS

Manfred M. KAPPES, Roland W. KUNZ\* and Ernst SCHUMACHER



## VARIATIONAL SPHERICAL MODEL OF SMALL METALLIC PARTICLES

J.L. MARTINS, R. CAR and J. BUTTET

We study the structural and electronic properties of simple metal clusters with a model based on the density functional formalism. Our model takes into account electron relaxation effects and the lattice structure through the

$$IP(R) = WF + 1/2R, \quad EA(R) = WF - 1/2R,$$

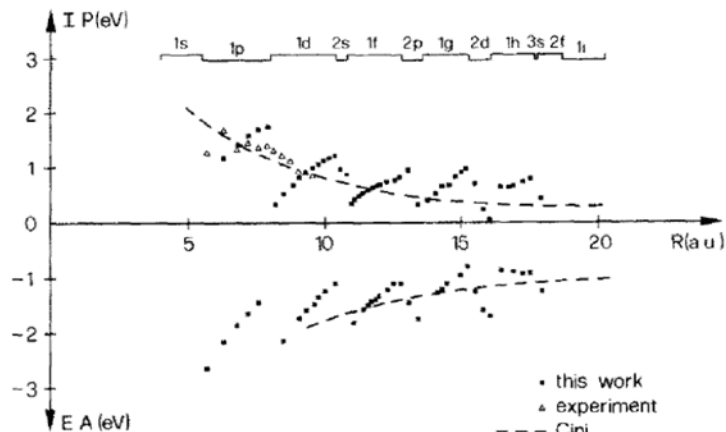


Fig. 1. Ionization potential and electron affinity of Na clusters as a function of the particle radius. The squares are the

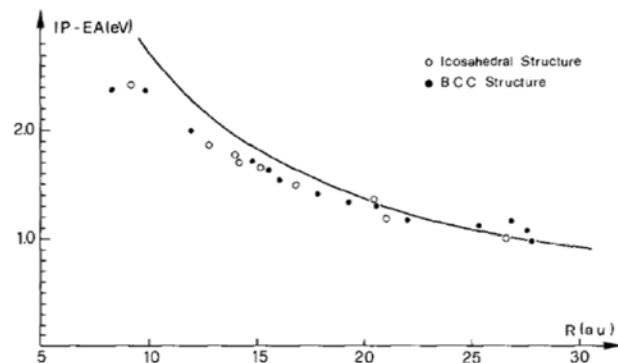
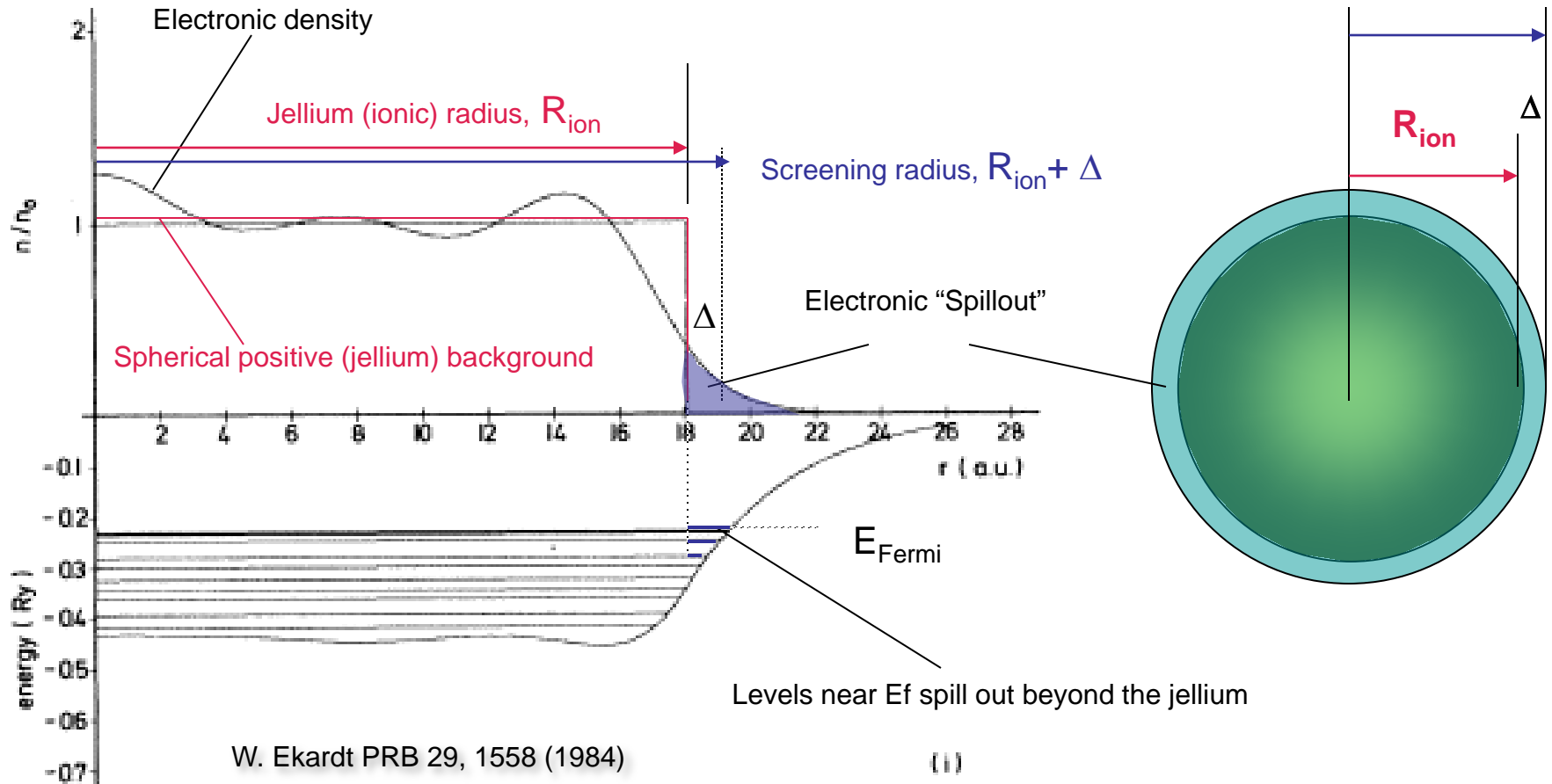


Fig. 2. Difference between the ionization potential and the electron affinity as a function of the particle radius. These results were obtained with the pseudopotential model and an uniform lattice relaxation. The full line is the  $1/R$  curve given by the electrostatic model. The cluster radius is defined as that of the spherical jellium model, i.e. the radius of a uniform spherical background of positive charge having the bulk metal density.

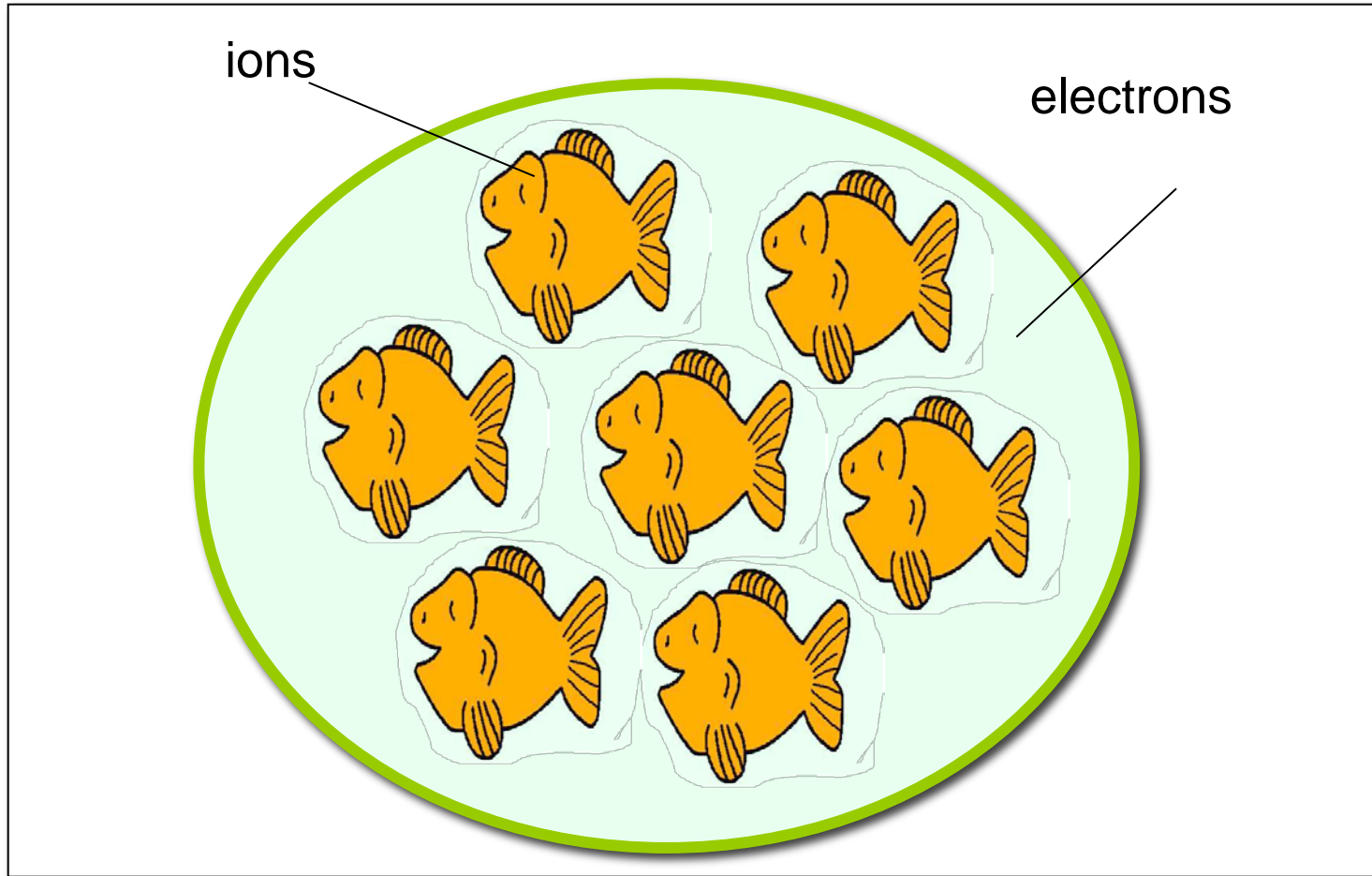


# The spherical jellium model



- + *Electronic structure in a positively charged sphere solved self consistently.*
- + *It "builds in" metallicity.*
- *Does not resolve shell discrepancies*

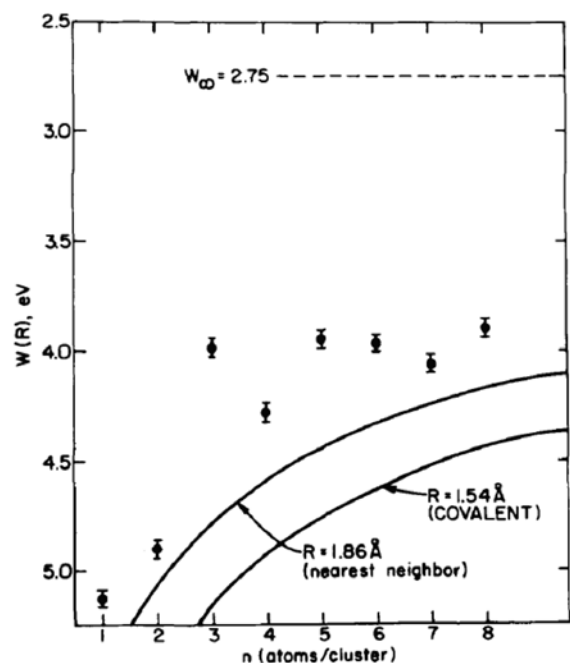
***That can be summarized as follows:  
Alkali clusters are like fish in a liquid droplet***



***The liquid, not the fish determines the shape of the droplet!***

# Photoionization of sodium clusters

K. I. Peterson,<sup>a)</sup> P. D. Dao, R. W. Farley, and A. W. Castleman, Jr.<sup>b)</sup>



Clearly, there are many unexplained and surprising facets regarding both the neutral and cluster ions and the field of metal cluster research deserves additional attention by both theoreticians and experimentalists. We can expect many important new and interesting findings to result.

1780

J. Chem. Phys. **80** (5), 1 March 1984

$$W(R) = W_\infty + \frac{3}{8} \frac{e^2}{R},$$

sodium lattice from x-ray data.<sup>16</sup> It is evident that the classical expression is not in very good accord with the experimental findings.

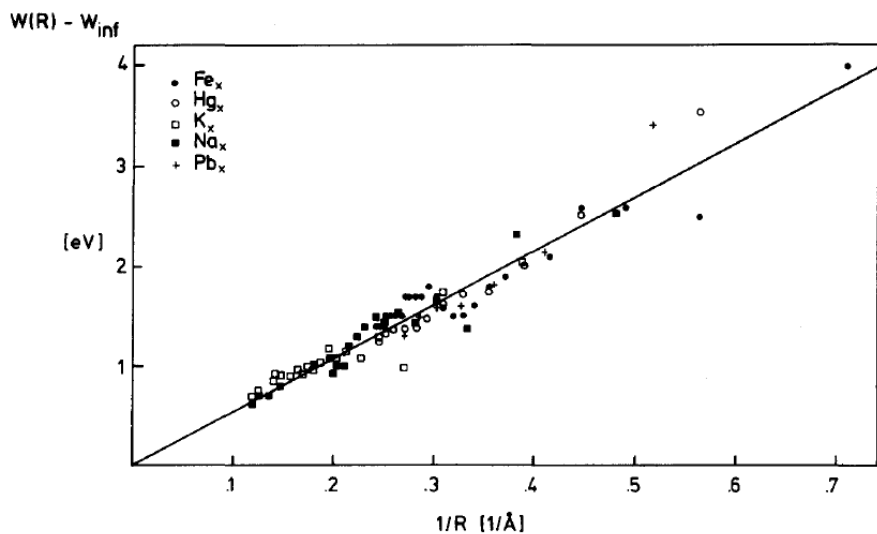
*Schumacher: Shell structure is right, but spherical jellium is not a good model in explaining other properties.*

J. Chem. Phys. **84** (3), 1 February 1986

## On the manifestation of electronic structure effects in metal clusters

Manfred M. Kappes, Martin Schär, Peter Radi, and Ernst Schumacher

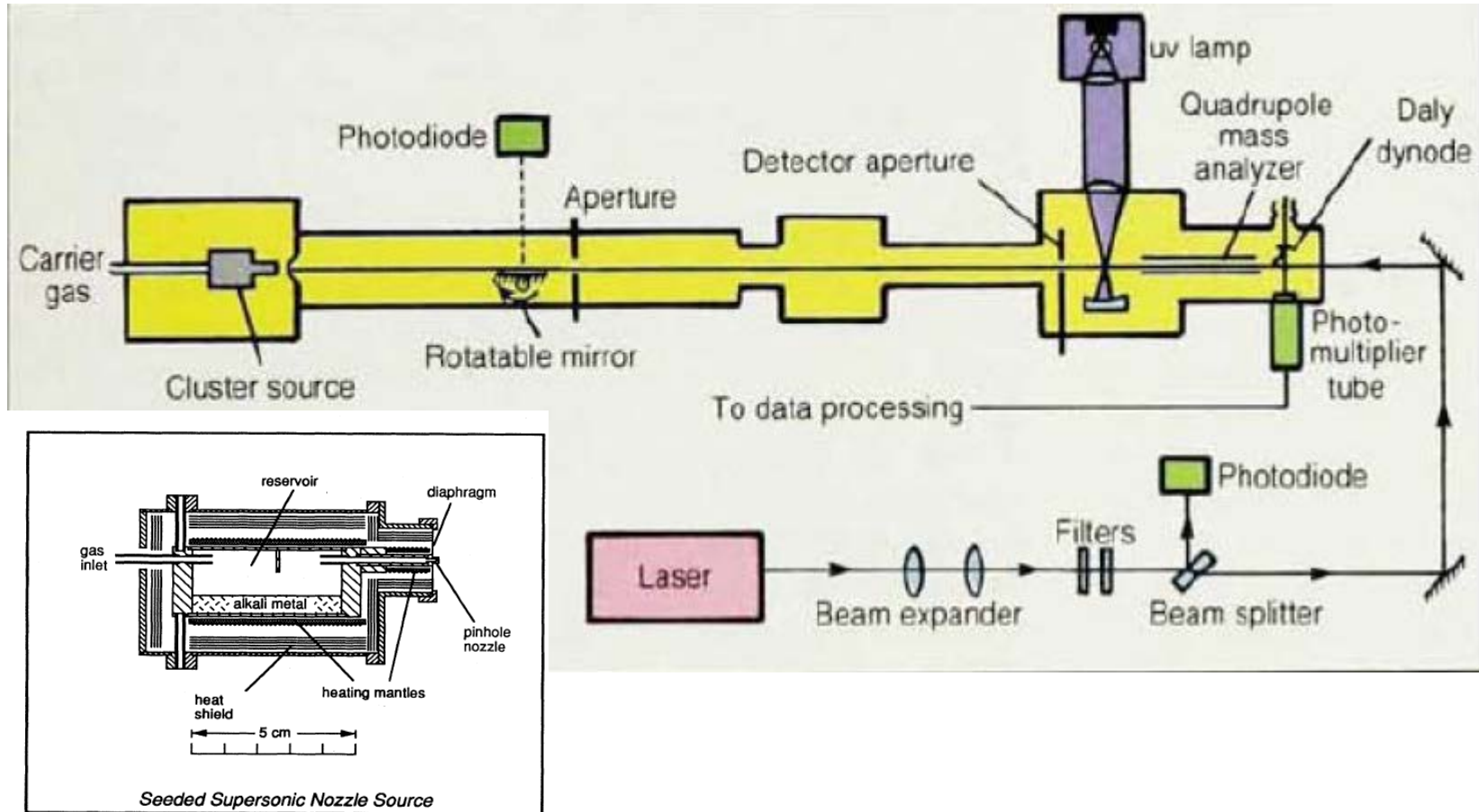
relative to neighboring clusters. We present data which show that a spherical jellium model, while providing a set of numbers correlating well with those of preferred stability in alkali clusters, is less successful in explaining other properties.



### C. Summary

The jellium model has served a useful function in pointing out and rationalizing a phenomenon which undoubtedly involves electronic structure effects. Its total neglect of geometrical structure and core (jellium) polarization is however no longer justifiable given the weight of opposing (quantitative) experimental evidence. We believe that there is no shortcut around serious quantum chemical calculations in this field. It would be damaging if the apparent success of the jellium model in rationalizing cluster abundances should jeopardize such endeavors.

*Knight's idea: molecular beam resonance experiments on very small clusters to explore "quantum size effects".*



## Electronic Shell Structure and Abundances of Sodium Clusters

W. D. Knight

Department of Physics, University of California, Berkeley, California 94720,<sup>(a)</sup>  
and Clarendon Laboratory, Oxford OX1 3PU, United Kingdom

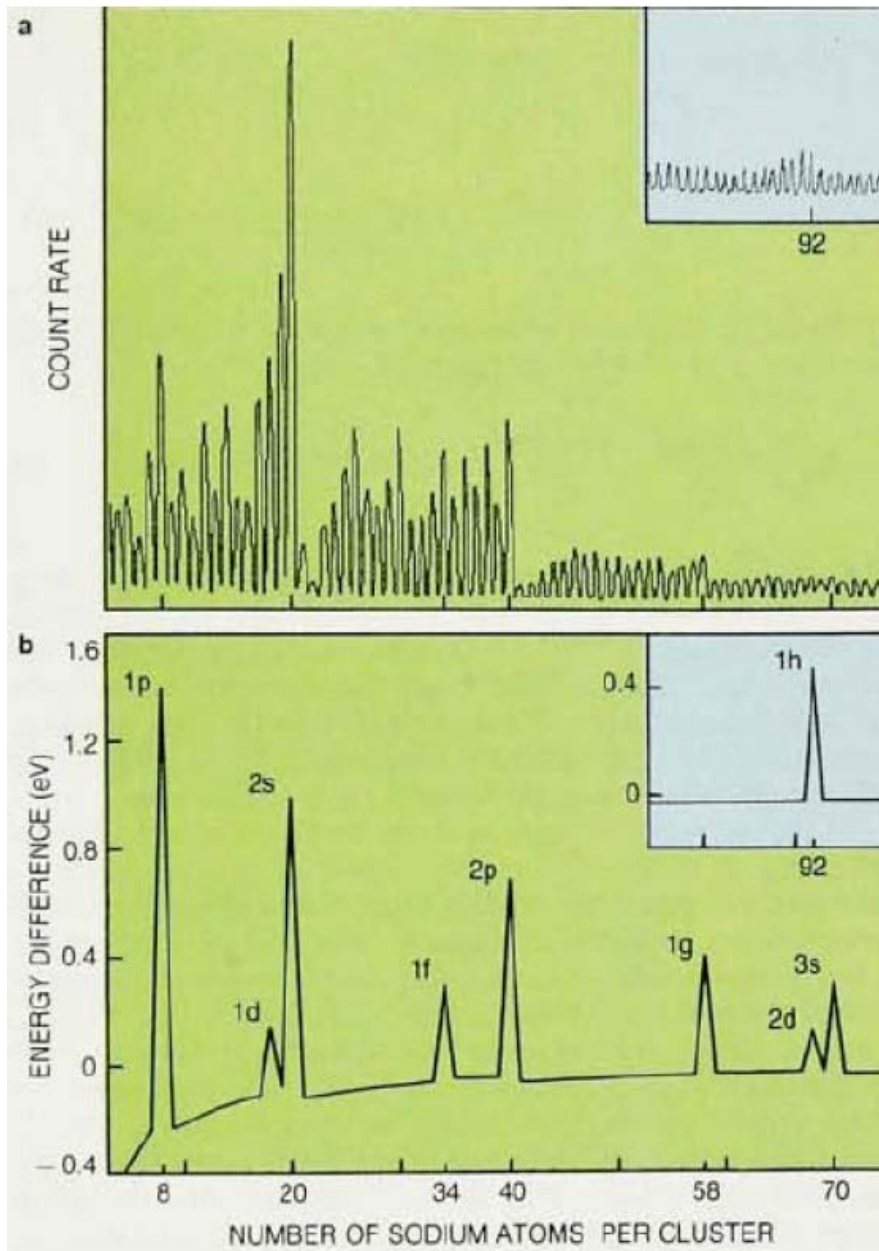
Keith Clemenger, Walt A. de Heer, and Winston A. Saunders  
Department of Physics, University of California, Berkeley, California 94720

M. Y. Chou and Marvin L. Cohen

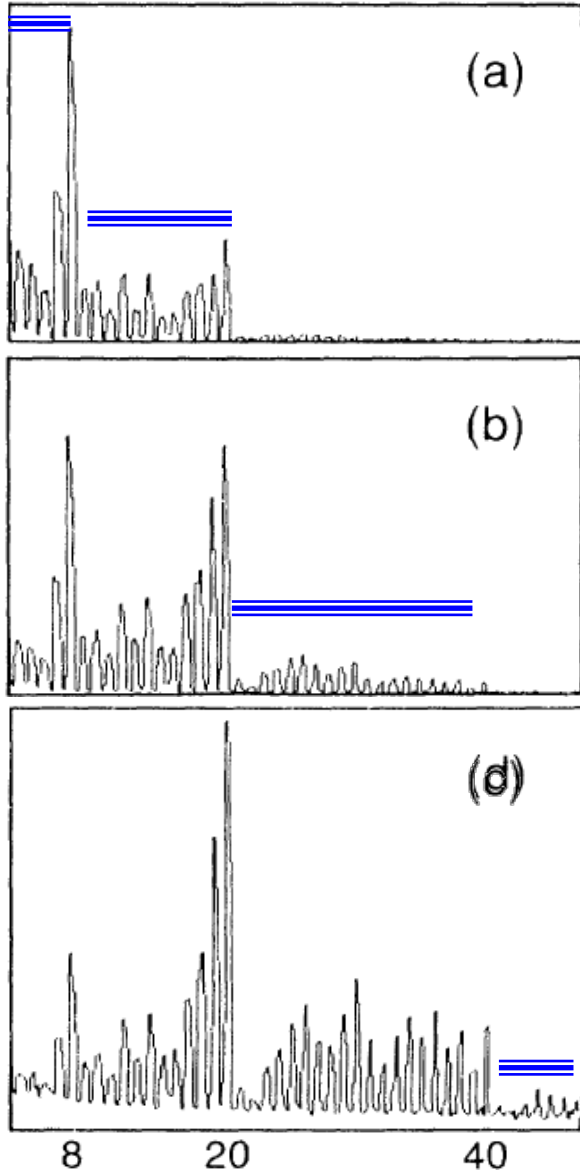
Department of Physics, University of California, Berkeley, California 94720, and Materials and Molecular Research Division,

*For a brief and accurate account of the discovery, see  
**Science News**, July 19, 2008 by Walt de Heer, Keith Clemenger,  
Winston A. Saunders, in response to story in  
**Science News**, June 21, 2008*

Abundance spectrum measured for Na clusters  
(a) compares favorably with the calculated second-order energy difference between neighboring clusters in a sequence (b).



# First indication of shells: the spectra evolve shell-by-shell



Increasing carrier gas pressure  
(increasing cooling)



FIG. 2. Sodium-cluster mass spectra ( $N = 4-47$ ) for varying carrier-gas pressure  $P_{Ar}$  at constant sodium vapor pressure 16 kPa. (a)  $P_{Ar} = 300$  kPa, (b)  $P_{Ar} = 400$  kPa, (c)  $P_{Ar} = 500$  kPa, and (d)  $P_{Ar} = 600$  kPa.

# Spherical potentials (delocalization)

De Heer, Rev. Mod. Phys. **65** 1993 611

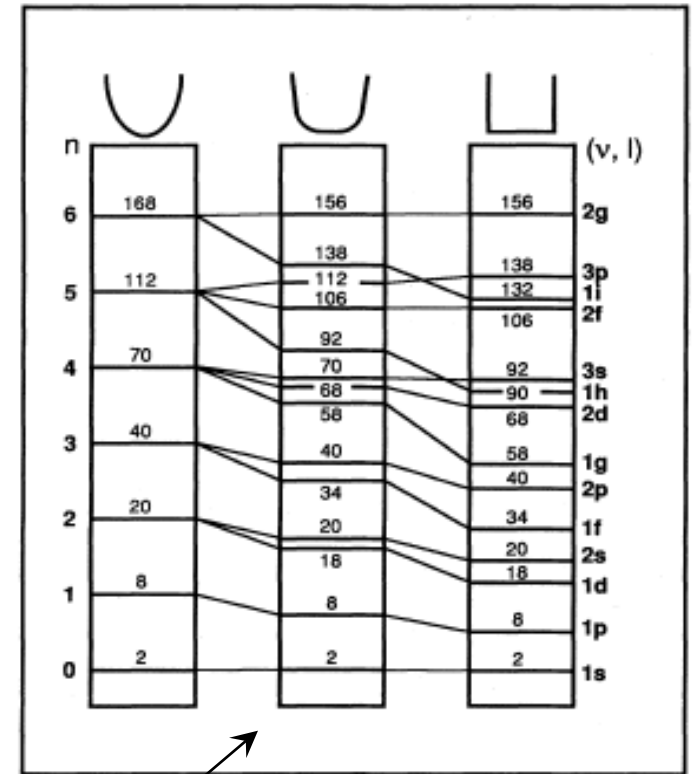
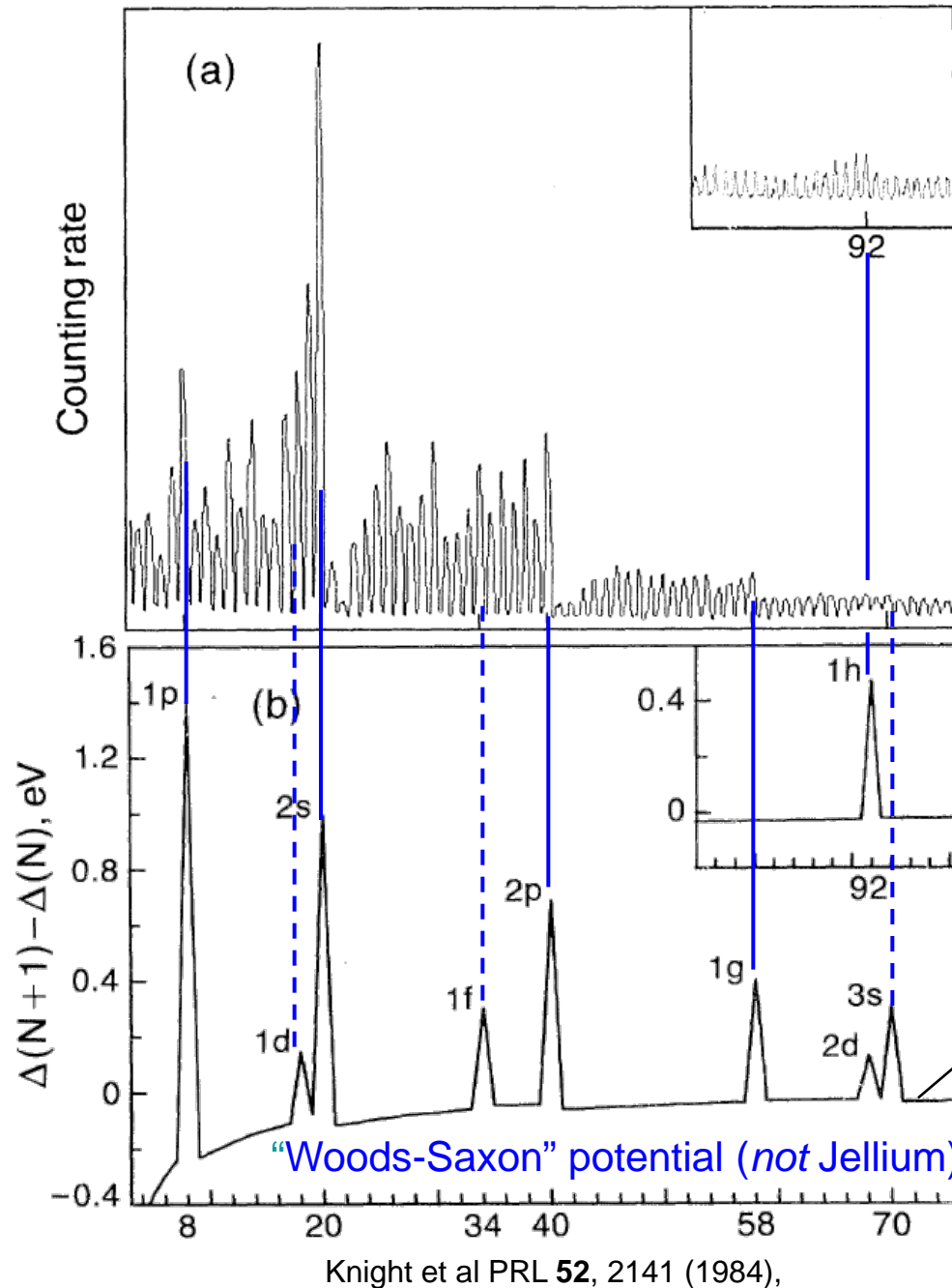


FIG. 2. Energy-level occupations for spherical three-dimensional, harmonic, intermediate, and square-well potentials. After Mayer and Jensen, 1955.

*Spherical potentials: produce shells, but discrepancies remain.*

Unlike in atoms, for the energy levels of clusters, there is no limitation between radial quantum number  $n$  and angular quantum number  $l$ , due to different confinement potentials



# Deep insight into the physics behind the shell structure

S. Bjornholm, J. Borggreen

Philosophical Magazine B, 1999 , **79**, 1321

## Nuclei and Metal Clusters:

- Although **the attractive forces** behind the formation of metallic medium and nuclear medium are totally different, they share the property of **being too weak to allow crystallization** of the electrons or the nucleons, respectively.
- In a crystal, each constituent is narrowly localized to its lattice position. This in turn implies a high zero-point energy, which the binding forces must be able to balance. If they cannot, the constituents will remain delocalized to the highest possible extent resulting in a liquid-like medium (the quantum liquid).
- In the bulk metal, the positive ions, being much heavier than the electrons, have considerably lower zero-point energies and hence for their part are able to form a crystal lattice.

# Shell structure versus the Jellium model

## *Shell Structure*

The property of [metal clusters] that [valence electrons] occupy quantum states which are in groups of approximately the same energy, called **shells**, the number of [valence electrons] in each shell being limited by the Pauli exclusion principle

[nuclei,

[similar nucleons,

atoms,

electrons,

metal clusters]

valence electrons]

## *Model*

A model is *a simplified* description of the complex reality *designed to reveal the main workings* of a system.

***Shell structure is a property, not a model!***

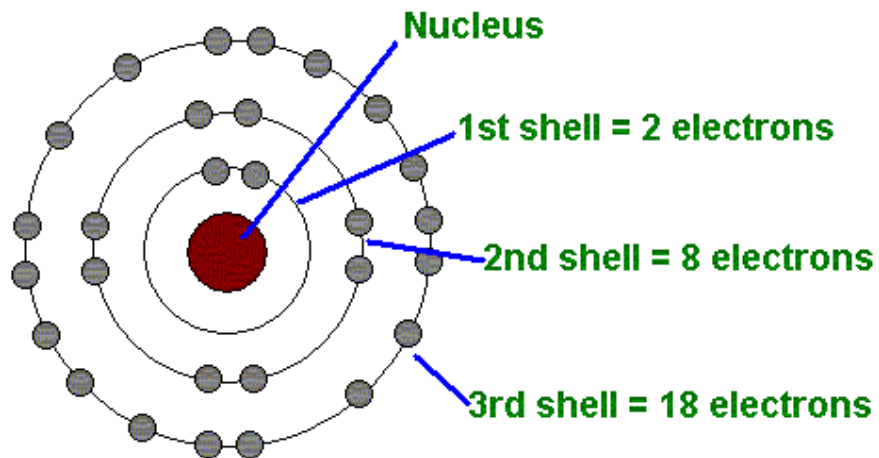
# Atomic Shell Structure

*Simplest Model:* Coulomb potential (Bohr atom)  
*Aufbau* with independent electrons.

*First order corrections:*

Many-body effects (screening): “Hunds Rules”;

*Shell closings (Periodic Table):* 2, 10, 18, 36, 54, 86



# Nuclear Shell Structure

## *Simplest model:*

3D harmonic potential;

Independent nucleons;

Magic Numbers:  $\Sigma(n+1)(n+2)$

→ 2, 8, 20, 40, 70, 112

## *First order corrections:*

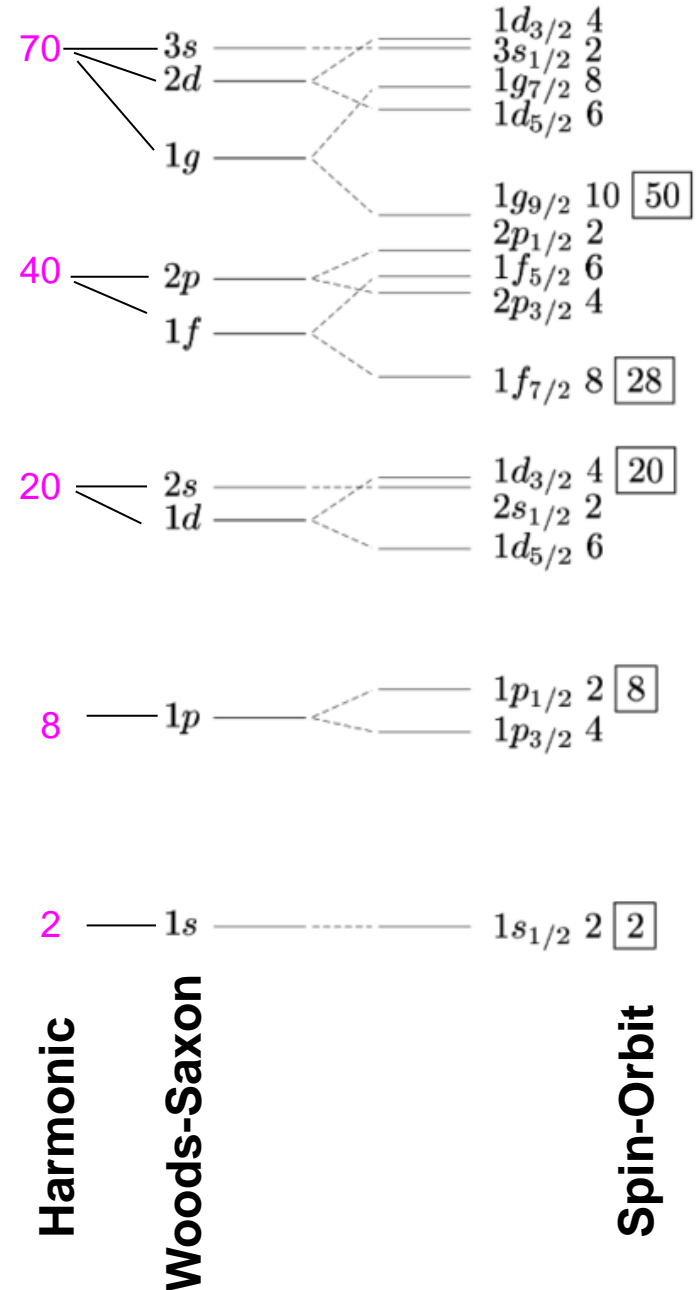
Spin-orbit coupling (Goeppert Mayer)

Rounded well (Woods-Saxon)

Ellipsoidal distortions (eg Nilsson)

## *Shell closings (Magic Numbers):*

2, 8, 20, 28, 50, 82, 126



# Shell Structure in Alkali Clusters

## *Simplest model:*

3D isotropic harmonic potential

Independent electrons

Magic Numbers:  $\Sigma(n+1)(n+2) \rightarrow 2, 8, 20, 40, 70, 112$

## *First order corrections:*

Rounded ellipsoidal well (Nilsson-Clemenger)

Major Shell closings: (2, 8, 20, 40, 58, 92)

Sub Shell closings: 10, 14, 18, 26, 30, 34, 50, ...

# Nilsson Hamiltonian (spheroidal model)

Harmonic oscillator potential

Anharmonic correction

$$H = \frac{\mathbf{p}^2}{2m} + \frac{m\omega_0^2\mathbf{q}^2}{2} - U\hbar\omega_0[l^2 - n(n+3)/6],$$

$p, q$  single-electron momentum and position

$l$ : angular momentum

$U$ : anharmonic amplitude

$n$ : shell index

$$R_0 = r_s N^{1/3}$$

$$\hbar\omega_0 = E_F / N^{1/3}$$

where  $p$  and  $q$  are single-electron momentum and coordinate operators,  $l$  is the angular momentum, and  $n$  is the shell number. The third, anharmonic correction term modifies the shape of the well and is constructed to keep the average shell energy constant. The spatial extent of the electronic charge density  $\langle r^2 \rangle$  is determined by the shape of the well and by the oscillator frequency  $\omega_0$  (see also Clemenger, 1985 and de Shalit and Feshbach, 1974, pp. 194–199). Relating  $\langle r^2 \rangle$  to the size of the cluster,  $R_0 = r_s N^{1/3}$  fixes  $\hbar\omega_0 = E_F / N^{1/3}$ , where  $E_F$  is the bulk Fermi energy and  $r_s$  is the Wigner-Seitz radius.

# Anharmonic Spheres

$$H = \frac{\mathbf{p}^2}{2m} + \frac{m\omega_0^2\mathbf{q}^2}{2} - U\hbar\omega_0[l^2 - n(n+3)/6]$$

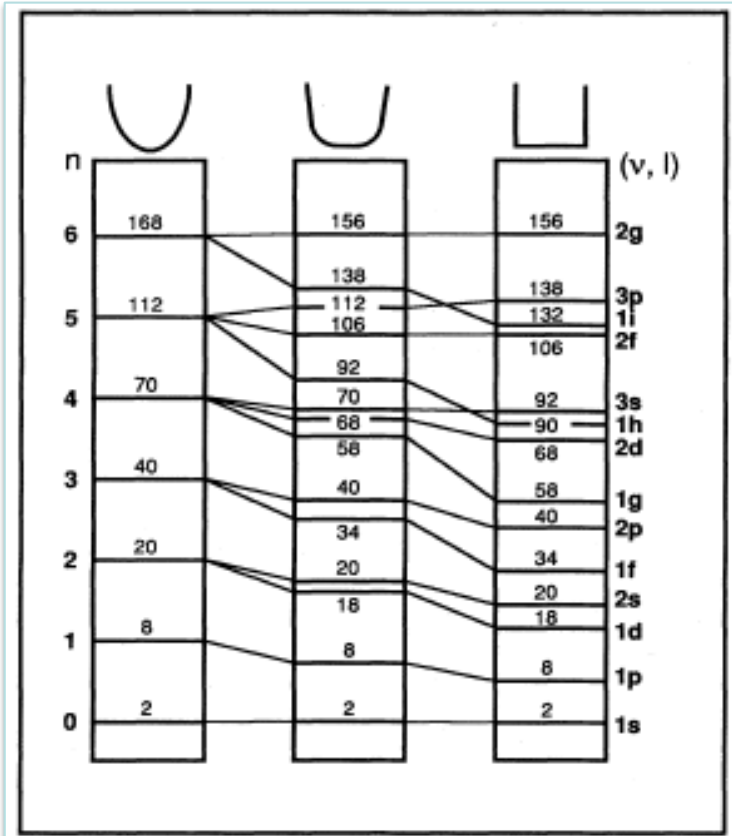
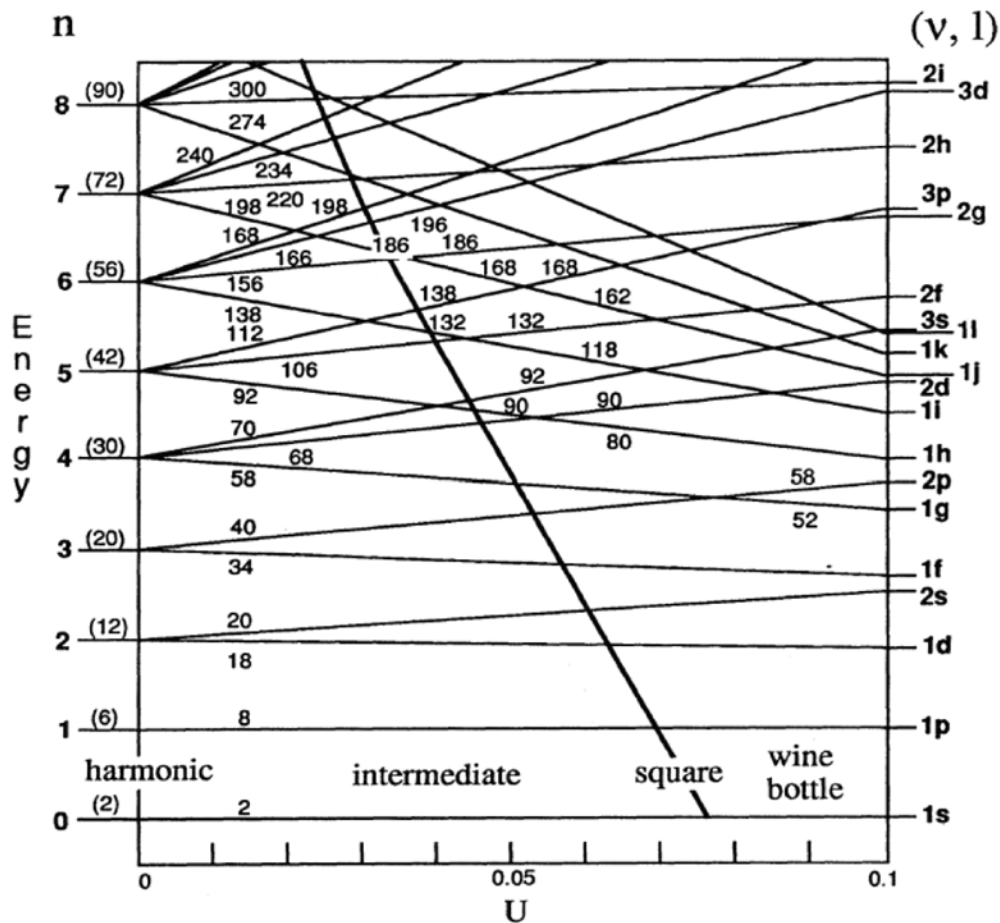
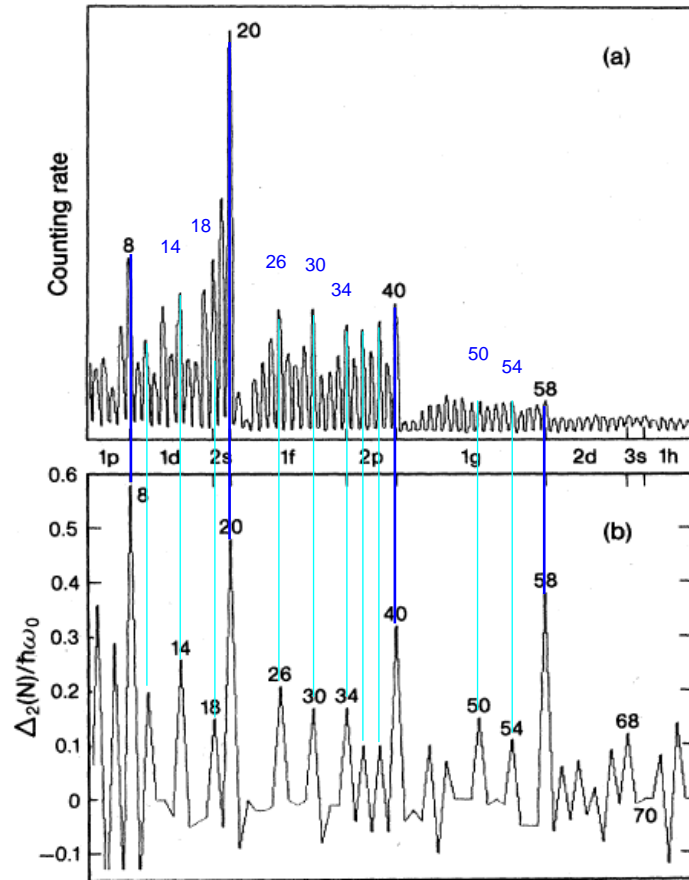


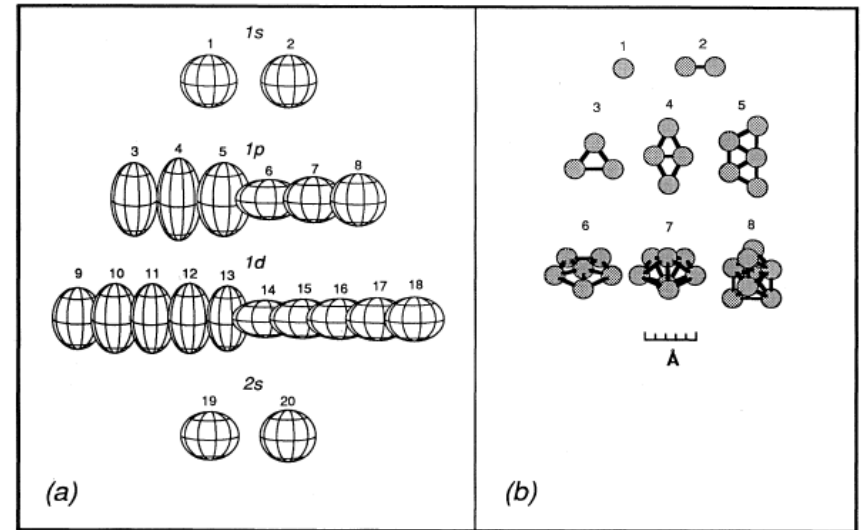
FIG. 2. Energy-level occupations for spherical three-dimensional, harmonic, intermediate, and square-well potentials. After Mayer and Jensen, 1955.

# Anharmonic spheres with spheroidal distortions: Spheroidal electron droplet model

*Cluster shapes are determined by the electronic structure*



Clemenger, PRB **32** 1359 (1985)

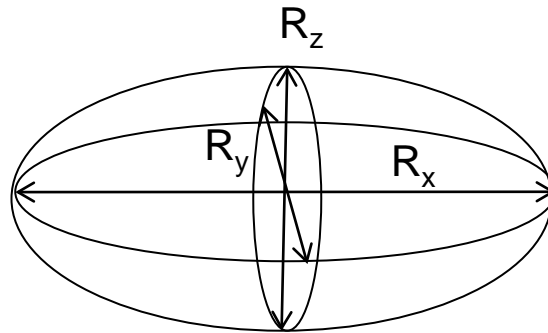


- + *Simplified description that reveals the main workings*
- + *Resolves shell edge discrepancies of spherical models.*



# 3D harmonic oscillator model with ellipsoidal distortions (easy to calculate)

$$H = \frac{\mathbf{p}^2}{2m} + \frac{m\omega_0^2 \mathbf{q}^2}{2}$$



Single particle energies

$$E_{n_x, n_y, n_z} = \hbar\omega_0 R_0 [(n_x + 1/2)/R_x + (n_y + 1/2)/R_y + (n_z + 1/2)/R_z]$$

## Total Energies

$$E_{\text{tot}} = h\omega_0 \sum_{\text{occ}} \left[ (n_x + \frac{1}{2}) \frac{R_0}{R_x} + (n_y + \frac{1}{2}) \frac{R_0}{R_y} + (n_z + \frac{1}{2}) \frac{R_0}{R_z} \right]$$
$$= h\omega_0 R_0 \left[ \frac{C_x}{R_x} + \frac{C_y}{R_y} + \frac{C_z}{R_z} \right],$$

where  $R_x R_y R_z = R_0^3 = N r_s^3$ . It is trivial to find the  $\epsilon$

$$C_x = \sum_0^{n_x \text{ max}} (n_x + 1/2)$$

# Total Energy Surfaces

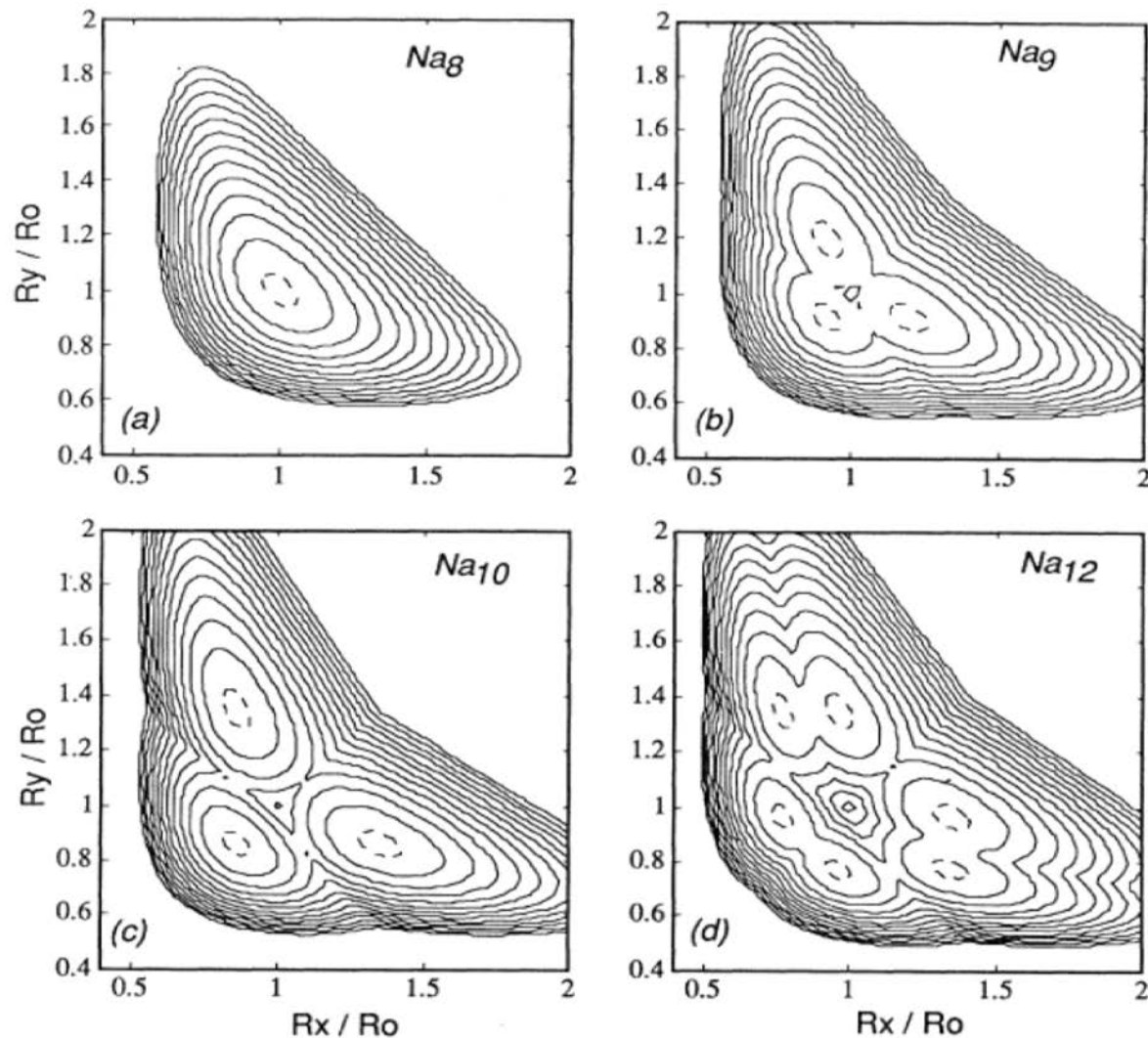


FIG. 55. Total-energy surfaces of several sodium clusters as a function of  $R_x$  and  $R_y$ , calculated in the ellipsoidal shell model. Contours are spaced every 0.2 eV. The dashed line corresponds to the 0.025-eV (room-temperature) contour.  $Na_8$  is spherical,  $Na_9$  and  $Na_{10}$  are spheroidal, and  $Na_{12}$  is ellipsoidal. From these figures the extent of the thermal tails in photoionization efficiency spectra are estimated as described in the text.

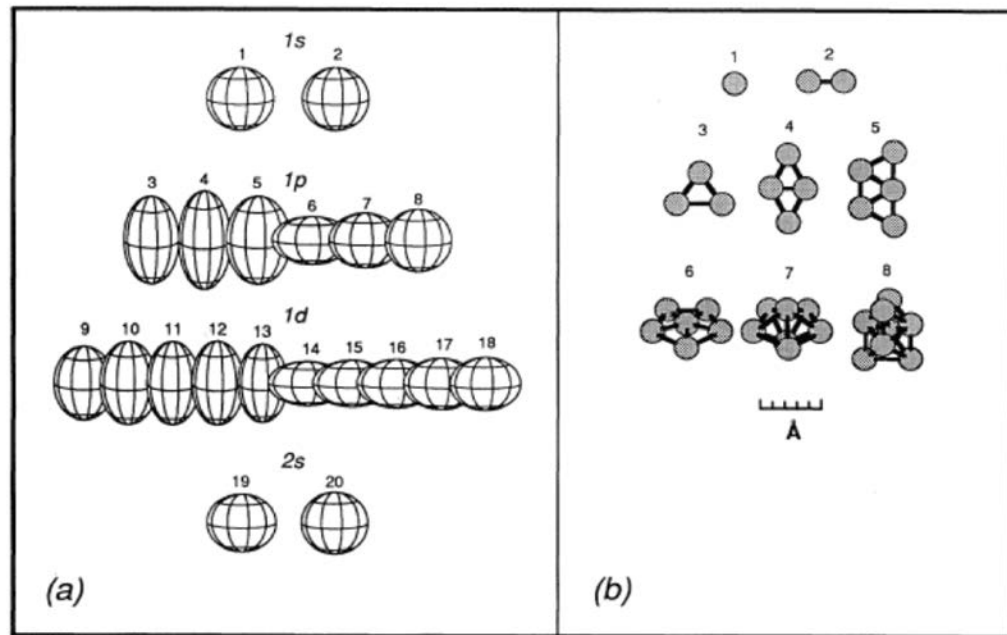
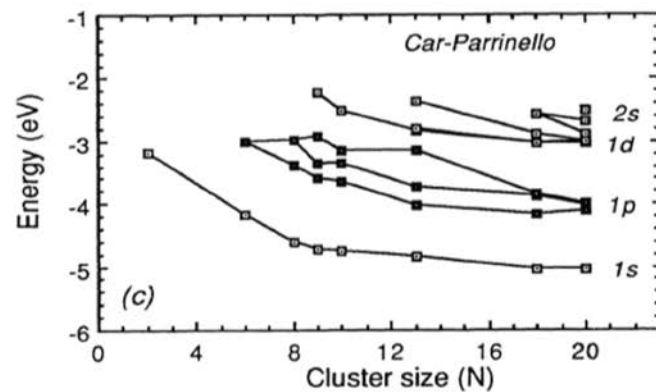
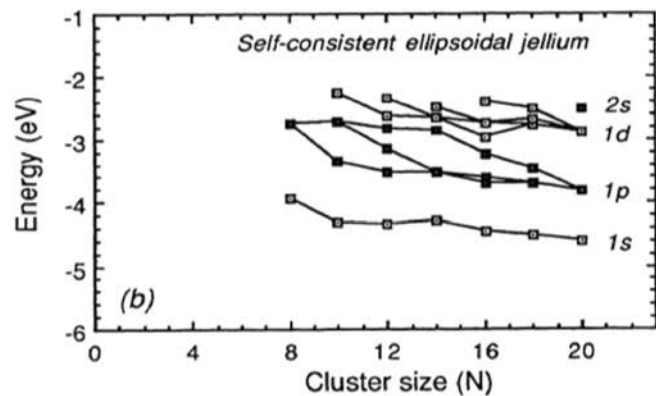
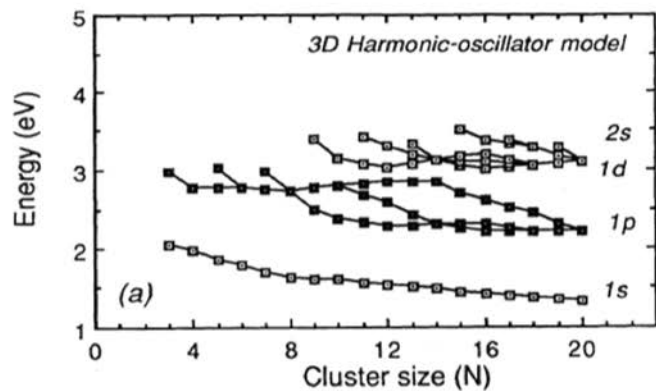
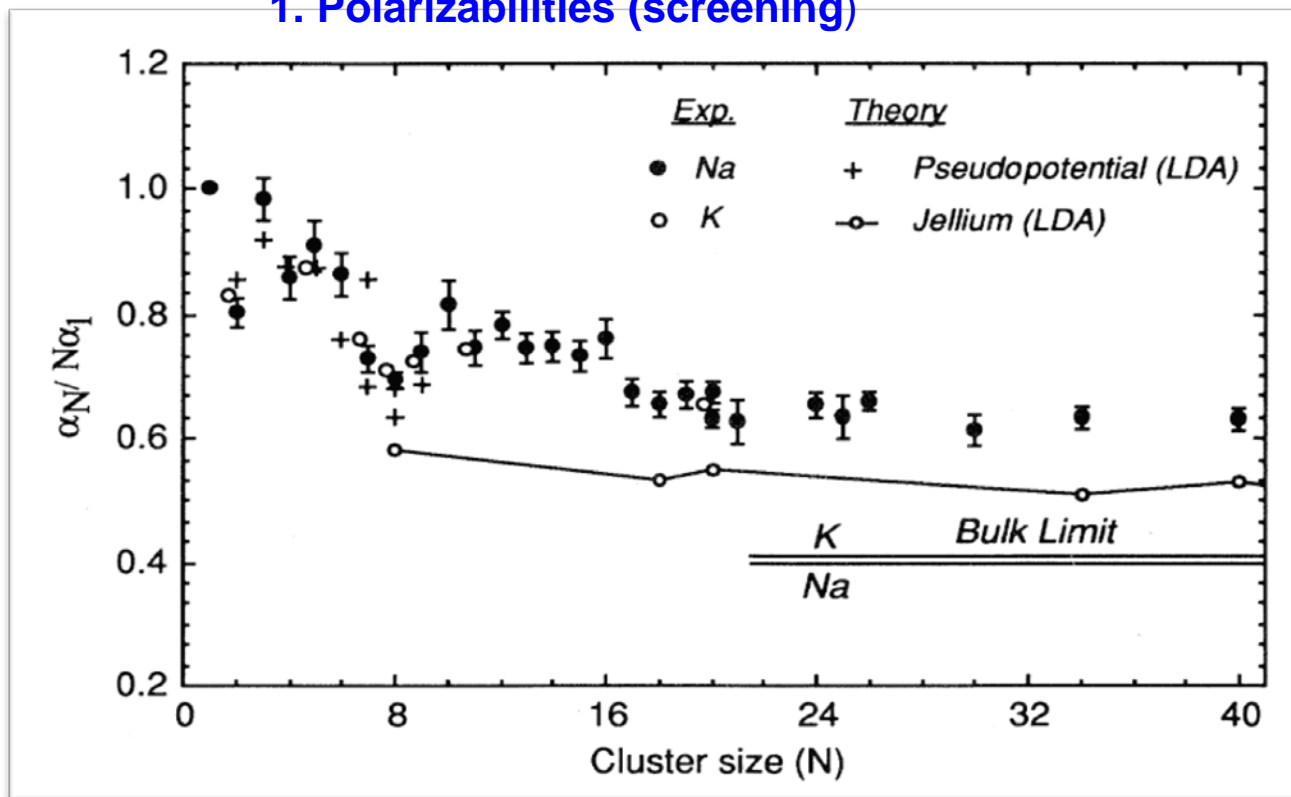


FIG. 54. Energy eigenvalues from the ellipsoidal shell (Clemenger-Nilsson) model: (a) the self-consistent spheroidal jellium calculations (from Lauritsch *et al.*, 1991); (b) the Car-Parrinello molecular-dynamics calculations (from R othlisberger and Andreoni, 1991).

# Early measurements of metallic properties of clusters

## 1. Polarizabilities (screening)



Knight, W. D., K. Clemenger, W. A. de Heer, and W. A. Saunders, 1985a, Phys. Rev. B **31**, 2539.

Saunders, W. A., K. Clemenger, W. A. de Heer, and W. D. Knight, 1985, Phys. Rev. B **32**, 1466.

de Heer, W. A., K. Selby, V. Kresin, J. Masui, M. Vollmer, A. Chatelain, and W. D. Knight, 1987, Phys. Rev. Lett. **59**, 1805.

W.A.de Heer, Rev. Mod. Phys. **65** 611, (1993)

# Ionization potentials of large Na clusters

## 2. Ionization potentials (Fermi level, screening )

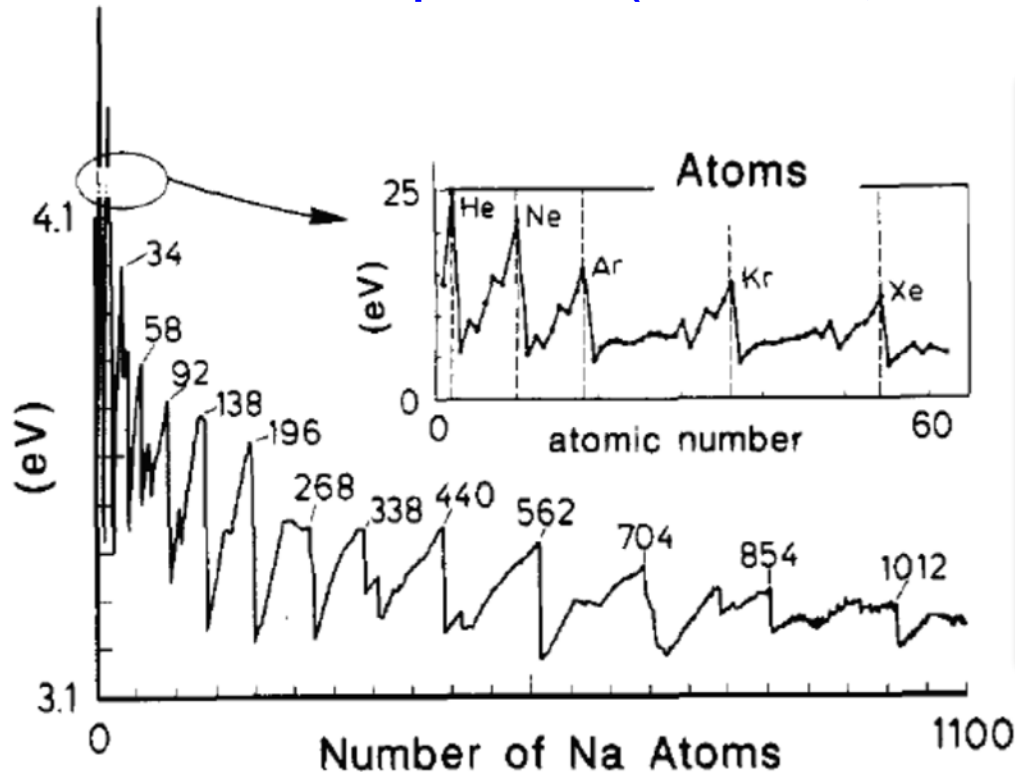
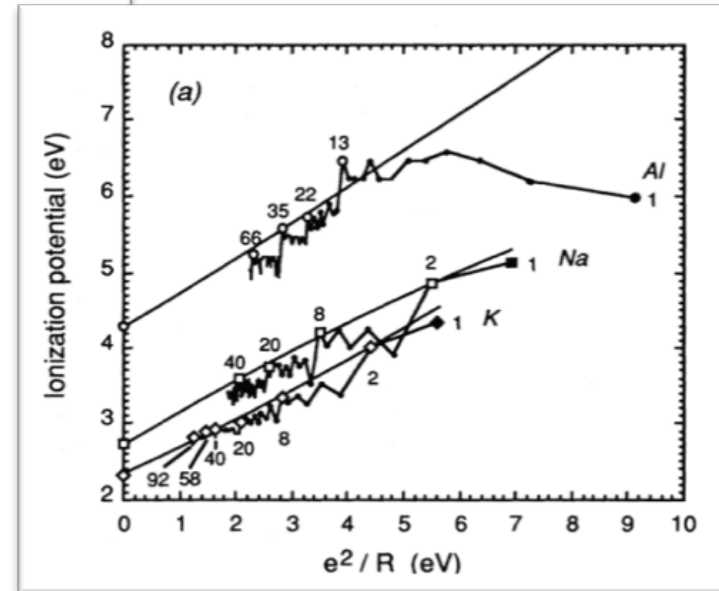


**Figure 10.** Ionization potentials calculated as a function of  $n$  for  $(\text{Na})_n$  clusters. A positive background charge distribution slightly concentrated in the central region has been used. Notice the similar behavior of the ionization energies of the chemical elements (inset).



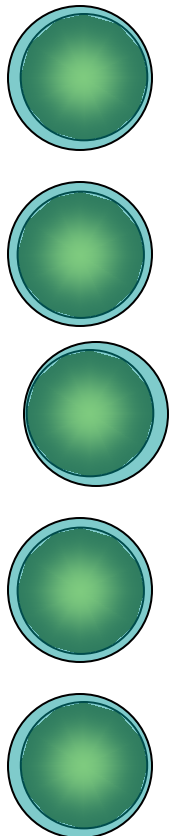
# Plasma resonances (electron-drop dominated shapes)

## Collective Dipole Oscillations in Small Sodium Clusters

Walt A. de Heer, Kathy Selby, Vitaly Kresin, Jun Masui, Michael Vollmer, A. Châtelain,<sup>(a)</sup>  
and W. D. Knight

*Department of Physics, University of California, Berkeley, California 94720*  
(Received 20 August 1987)

Photoabsorption cross sections of small neutral sodium clusters composed of  $N=2-40$  sodium atoms are measured by longitudinal-beam-depletion spectroscopy at several wavelengths of visible light. Absorption occurs via coupling of photons to collective oscillations of the valence electrons. The cross section is strongly size and wavelength dependent. Good agreement is found with predictions based on an extended Clemenger-Nilsson shell model and the experimental static polarizabilities.



Collective electron oscillations:  
(Very intense; almost exhaust the oscillator strength).

$$\omega = \frac{Q^2}{MR^3} = \frac{Q^2}{M\alpha^3}$$

$$M = Nm_e$$

$$Q = Ne$$

$$R = R_{ion} + \Delta$$

multiple peaks reflect non-spherical shapes)

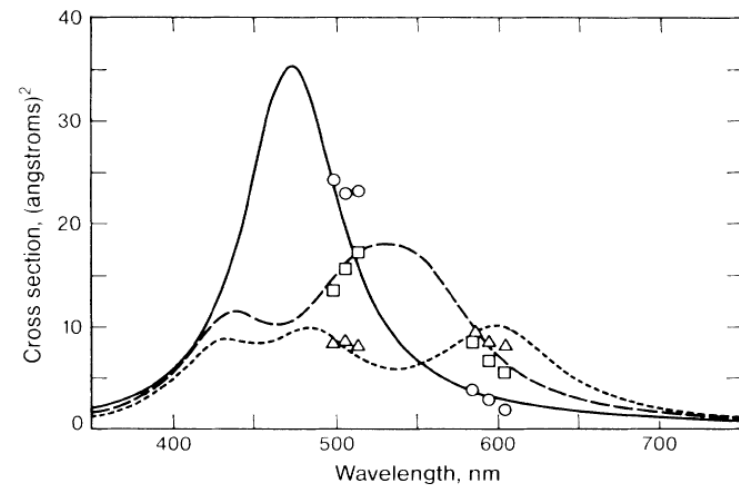


FIG. 3. Comparison of theoretical and experimental photoabsorption cross sections of sodium clusters.  $N=12$ : theory, short-dashed curve; experiment, triangles.  $N=16$ : theory, long-dashed curve; experiment, squares.  $N=20$ : theory, solid curve; experiment, circles. The multiple peaks of 12 and 16 are caused by ellipsoidal distortions. The damping constant is assumed to be  $0.15\omega_0$  for all clusters.

# Frank Condon overlap for photoelectron spectra 3D harmonic osc. model

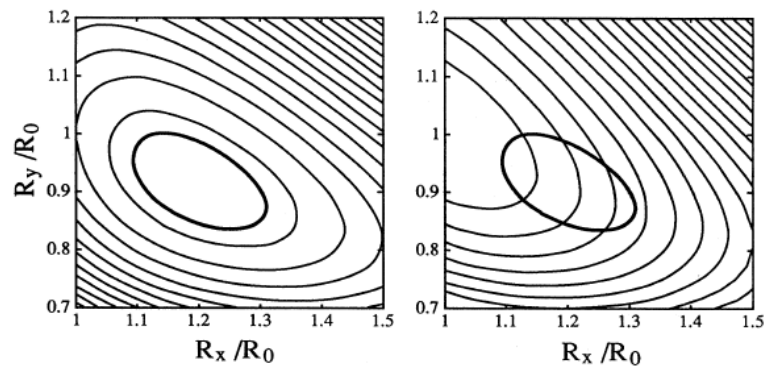
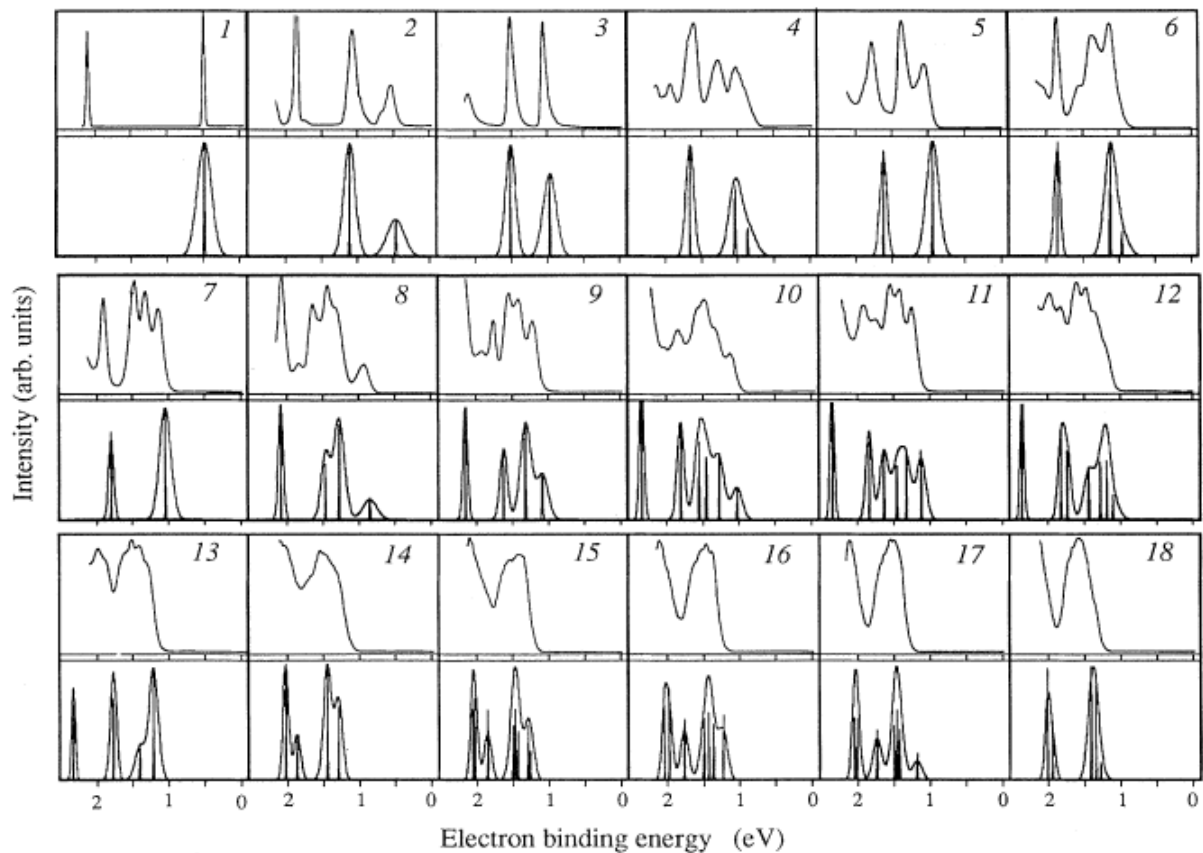


FIG. 59. Total-energy hypersurfaces for the quadrupole shape oscillations for the  $K_8^-$  cluster (left) and the  $K_8$  cluster (right).





# Shell structure around a hole: Alkali coated $C_{60}$

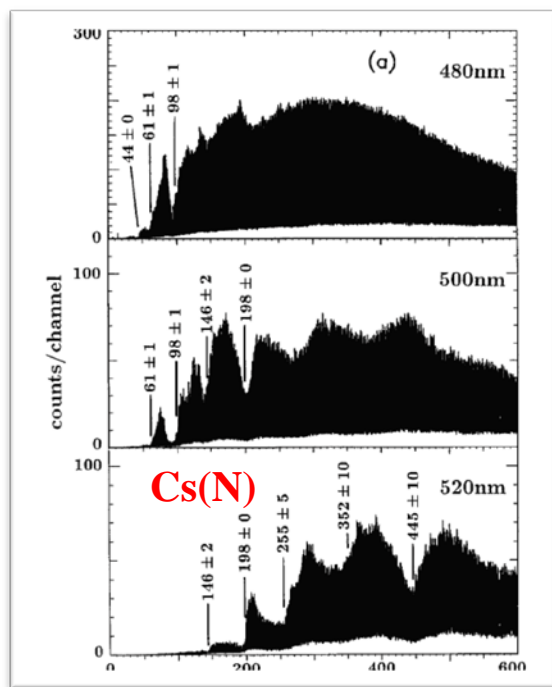
VOLUME 77, NUMBER 6

PHYSICAL REVIEW LETTERS

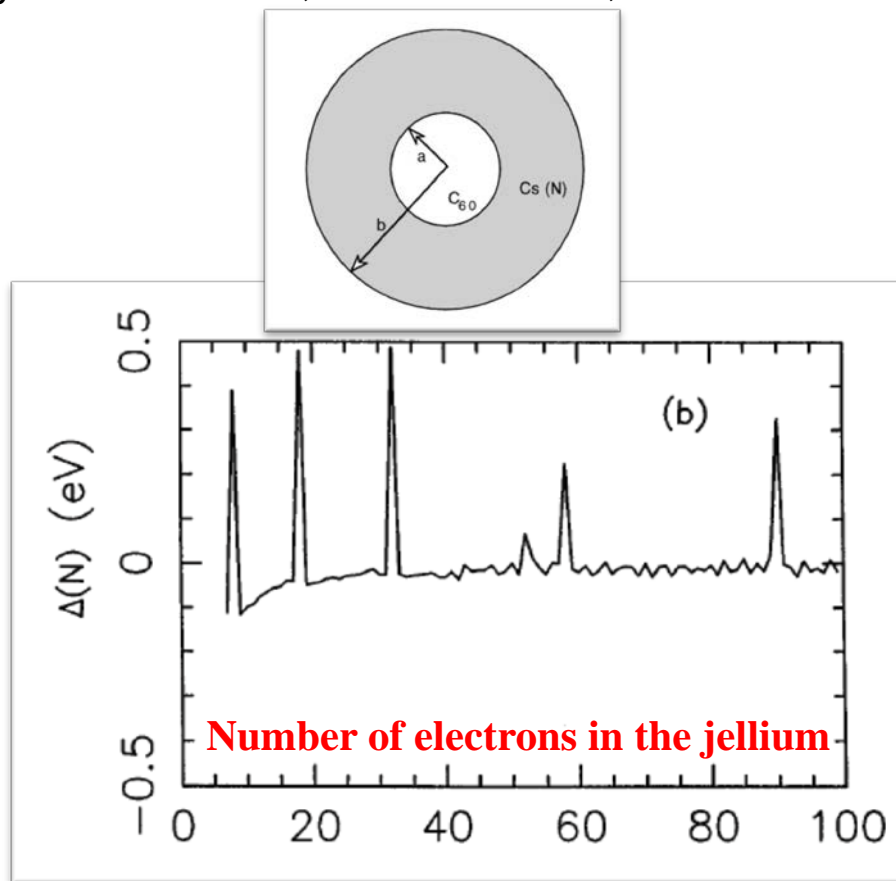
5 AUGUST 1996

## Electronic Shell Structure and Relative Abundances of Cesium-Coated $C_{60}$

M. Springborg, S. Satpathy, N. Malinowski, U. Zimmerman, T.P. Martin



Photoionization mass spectra of  $C_{60}/Cs(N)$  clusters with photons of various energies.



The total energy differences  $\Delta(N)$  calculated from DFT

# Magic nanoclusters of gold

A combination of theory and experiment is shedding new light on the structural and electronic properties of gold nanoclusters, including cage-like structures that contain other atoms.

**Pekka Pyykkö**

is in the Department of Chemistry and the Finnish Centre of Excellence in Computational Molecular Science, University of Helsinki, Helsinki, POB 55, 00014 Finland.

e-mail: [Pekka.Pyykko@helsinki.fi](mailto:Pekka.Pyykko@helsinki.fi)

nature nanotechnology | VOL 2 | MAY 2007 |

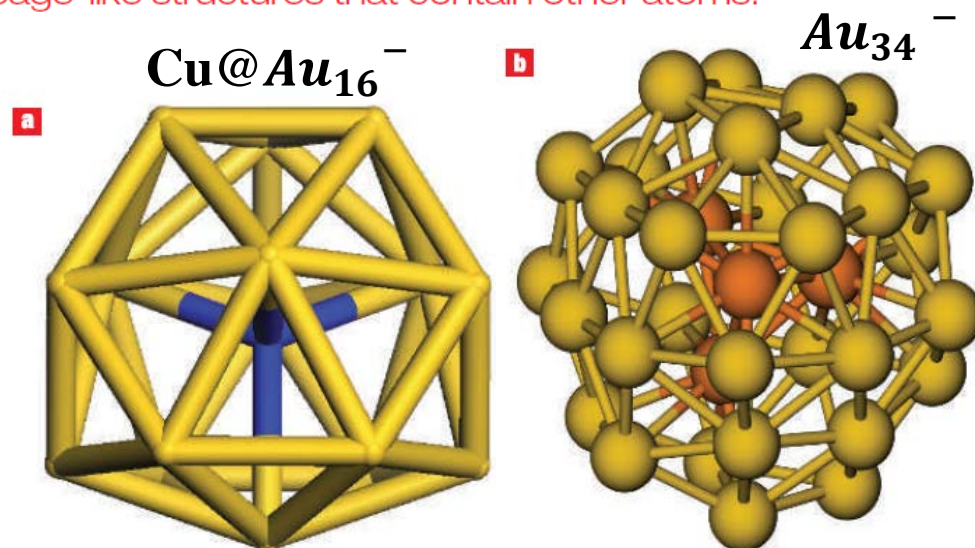


**Figure 1** Two types of stable gold clusters. **a**, Copper–gold clusters,  $\text{Cu@Au}_{16}^-$ , consisting of one copper atom (indicated schematically in blue) surrounded by a cage of sixteen gold atoms, have 18 valence electrons. Gold clusters with this ‘magic number’ of electrons tend to be very stable as it corresponds to filling the atomic-like *s*, *p* and *d* orbitals associated with the cluster<sup>6</sup>. **b**, Larger clusters with 34 atoms,  $\text{Au}_{34}^-$ , are also found to be stable, but have a much lower structural symmetry<sup>10</sup>.

# Oxidation-Resistant Gold-55 Clusters

H.-G. Boyen,<sup>1\*</sup> G. Kästle,<sup>1</sup> F. Weigl,<sup>1</sup> B. Koslowski,<sup>1</sup> C. Dietrich,<sup>1</sup>  
P. Ziemann,<sup>1</sup> J. P. Spatz,<sup>3</sup> S. Riethmüller,<sup>2</sup> C. Hartmann,<sup>2</sup>  
M. Möller,<sup>2</sup> G. Schmid,<sup>4</sup> M. G. Garnier,<sup>5</sup> P. Oelhafen<sup>5</sup>

Gold nanoparticles ranging in diameter from 1 to 8 nanometers were prepared on top of silicon wafers in order to study the size dependence of their oxidation behavior when exposed to atomic oxygen. X-ray photoelectron spectroscopy showed a maximum oxidation resistance for "magic-number" clusters containing 55 gold atoms. This inertness is not related to electron confinement leading to a size-induced metal-to-insulator transition, but rather seems to be linked to the closed-shell structure of such magic clusters. The result additionally suggests that gold-55 clusters may act as especially effective oxidation catalysts, such as for oxidizing carbon monoxide.

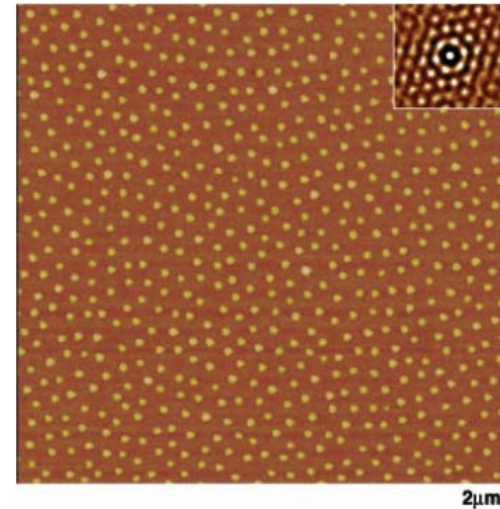
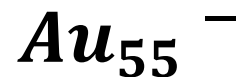


Fig. 1. AFM image of Au particles prepared by a micellar method (11) ( $z$  range, 20 nm). The inset shows the corresponding autocorrelation function indicating a high degree of hexagonal order. Analysis of the size distribution yields an average diameter of  $7.9 \pm 1.2$  nm.

# Au<sub>20</sub>: A Tetrahedral Cluster

Jun Li,<sup>1</sup> Xi Li,<sup>1,2</sup> Hua-Jin Zhai,<sup>1,2</sup> Lai-Sheng Wang<sup>1,2\*</sup>

Photoelectron spectroscopy revealed that a 20-atom gold cluster has an extremely large energy gap, which is even greater than that of C<sub>60</sub>, and an electron affinity comparable with that of C<sub>60</sub>. This observation suggests that the Au<sub>20</sub> cluster should be highly stable and chemically inert. Using relativistic density functional calculations, we found that Au<sub>20</sub> possesses a tetrahedral structure, which is a fragment of the face-centered cubic lattice of bulk gold with a small structural relaxation. Au<sub>20</sub> is thus a unique molecule with atomic packing similar to that of bulk gold but with very different properties.

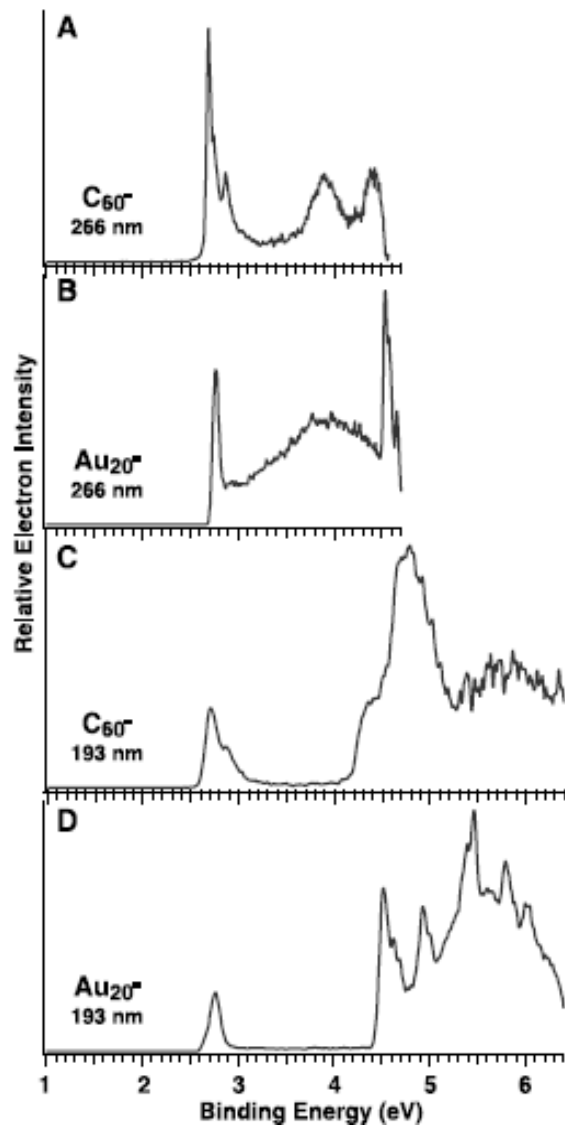


Fig. 2. Comparison of the photoelectron spectra of  $Au_{20}^-$  with those of  $C_{60}^-$ . (A) The 266-nm spectrum of  $C_{60}^-$ . "AD" stands for autodetachment signals. (B) The 266-nm spectrum of  $Au_{20}^-$ . (C) The 193-nm spectrum of  $C_{60}^-$ . (D) The 193-nm spectrum of  $Au_{20}^-$ .  $C_{60}^-$  data are from (24).

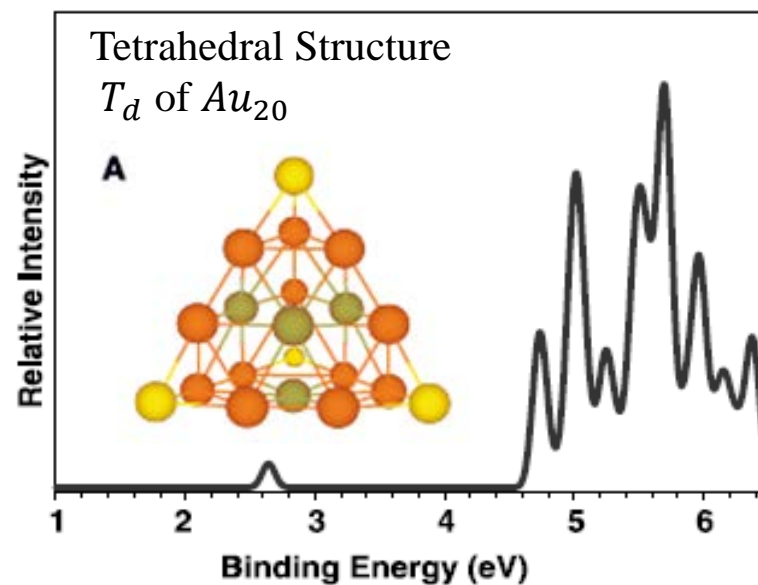


Fig. 4. The simulated photoelectron spectrum of  $Au_{20}^-$ . The simulated spectrum was constructed by fitting the distribution of the calculated detachment transition energies with unit-area Gaussian functions of 0.05 eV at full width at half maximum.

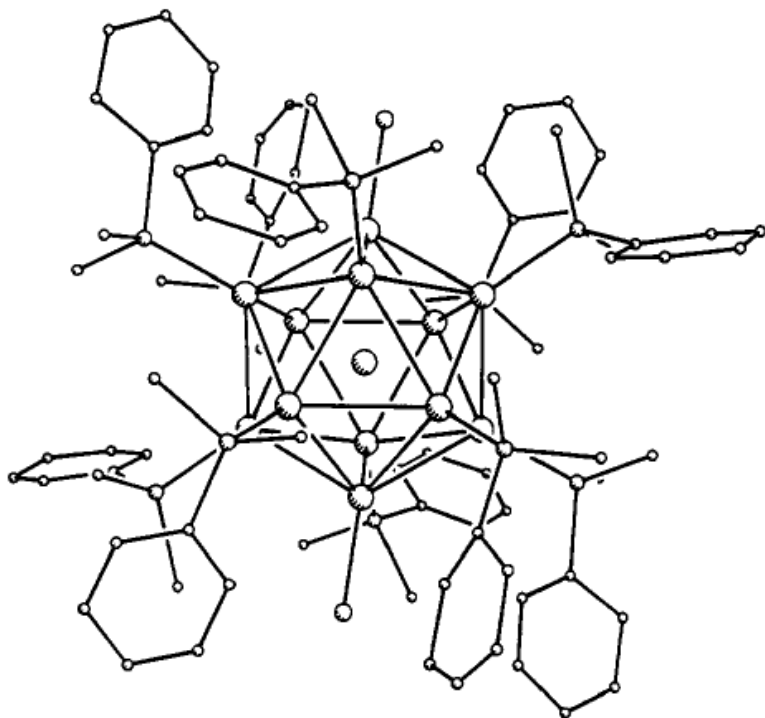
# Mackey $I_h$ series for TM

Chem. Rev. 1993, 93, 2693–2730

2693

## Chemical Catalysis by Colloids and Clusters

L. N. Lewis



*enectai*

*March*

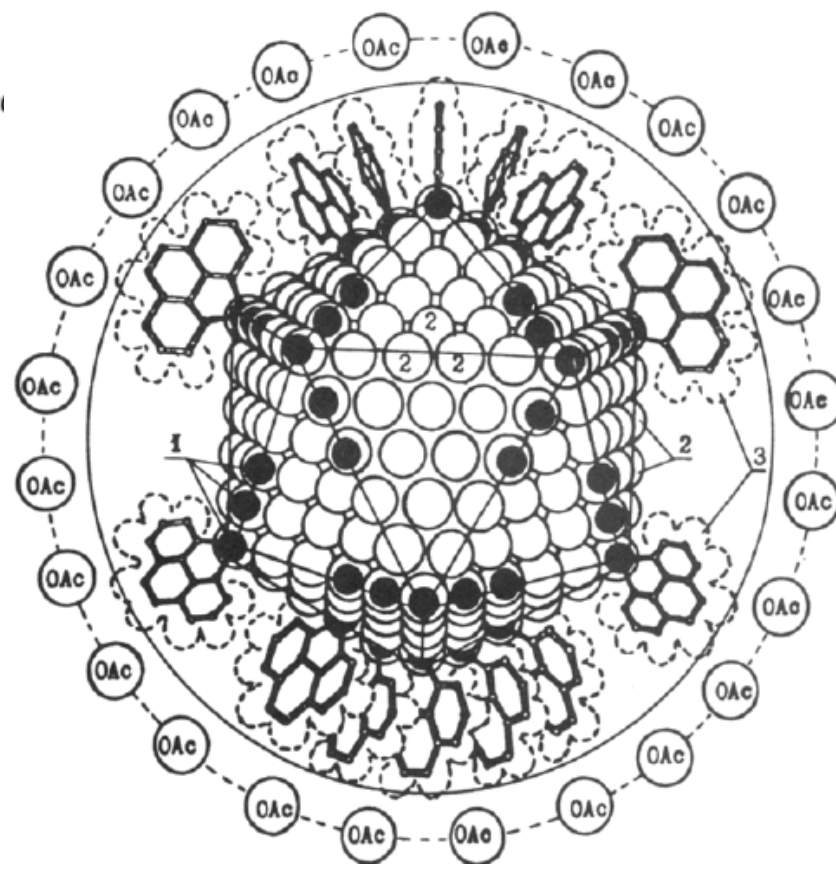
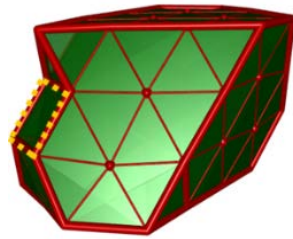
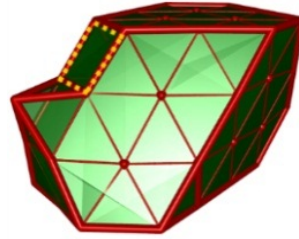


**Figure 1.** Example of a 13-atom icosahedral  $Au_{13}$  cluster. (Reprinted from ref 37; copyright 1988 Pergamon Press, Ltd.)

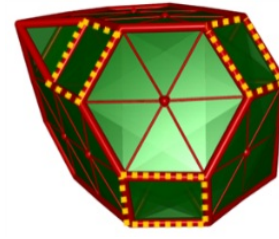
# Is $I_h$ - $TM_{55}$ (such as $Ru_{55}$ ) magic or non-magic?



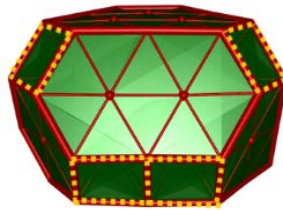
(A) -3.121



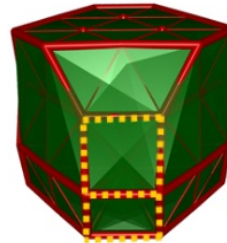
(B) -3.055



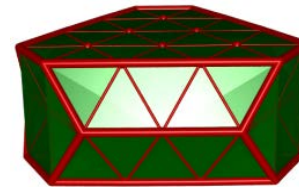
(C) -2.691



(D) -2.530



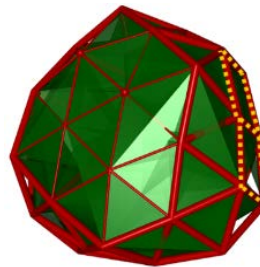
(E) -1.693



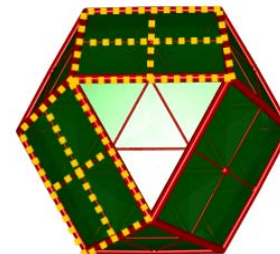
(F) -1.557



(G) 0.000



(H) 1.557



(I) 1.904

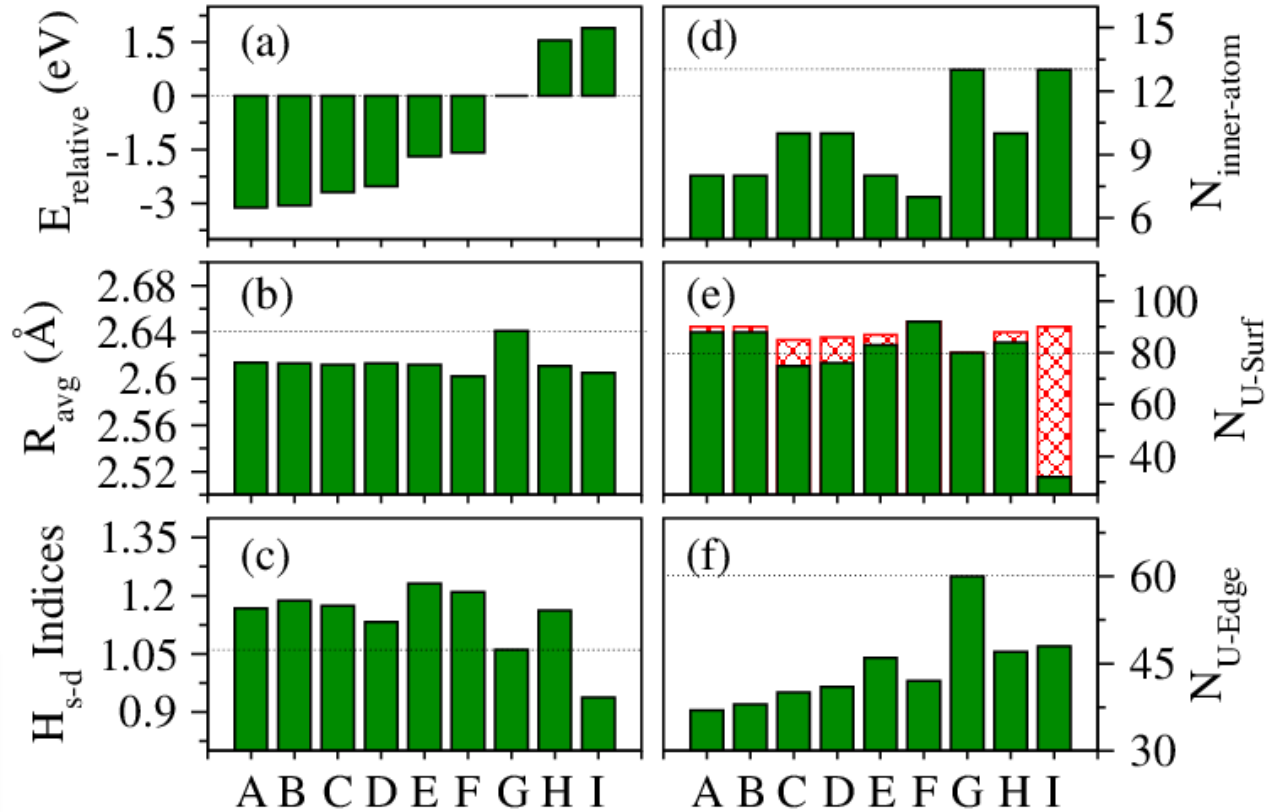
For  $Ru_{55}$ , the widely supposed stable candidates [icosahedron ( $I_h$ , the structure G), and octahedron (the structure I)] are actually dramatically less stable!

# What is the mechanism that stabilizes these more stable structures ?

The Wulff construction is a method for determining the equilibrium shape of a droplet or crystal of fixed volume inside a separate phase. Energy minimization arguments are used to show that certain crystal planes are preferred over others, giving the crystal its shape.

**Wulff Construction doesn't work!**

**Edge energy plays the key role!**



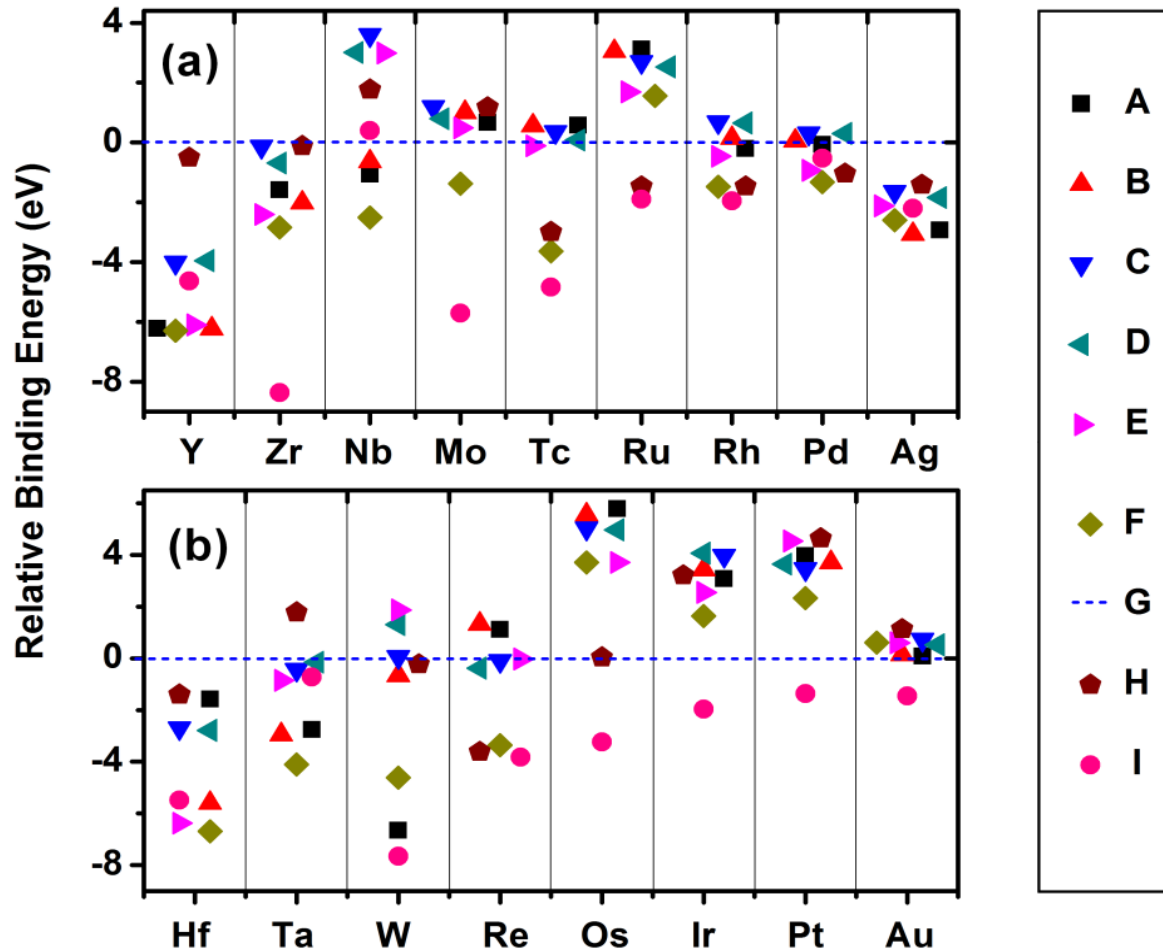
$$E_{tot} = E_{bulk} + E_{surf} + E_{edge} = N \times E_{avg-bulk} + S \times \alpha_{avg} + L \times \beta_{avg} \quad (1)$$

$$E_{surf} = \sum_i^n N_i a_i b_i \gamma_{ic} \dots\dots\dots(2)$$

$$E_{edge} = \sum_i^n N_i R_i \beta_i = \sum_i^n L_{i(hkl-uvw)} \beta_{avg} = N_{(U-Edge)} R \beta_{avg} \dots(3)$$

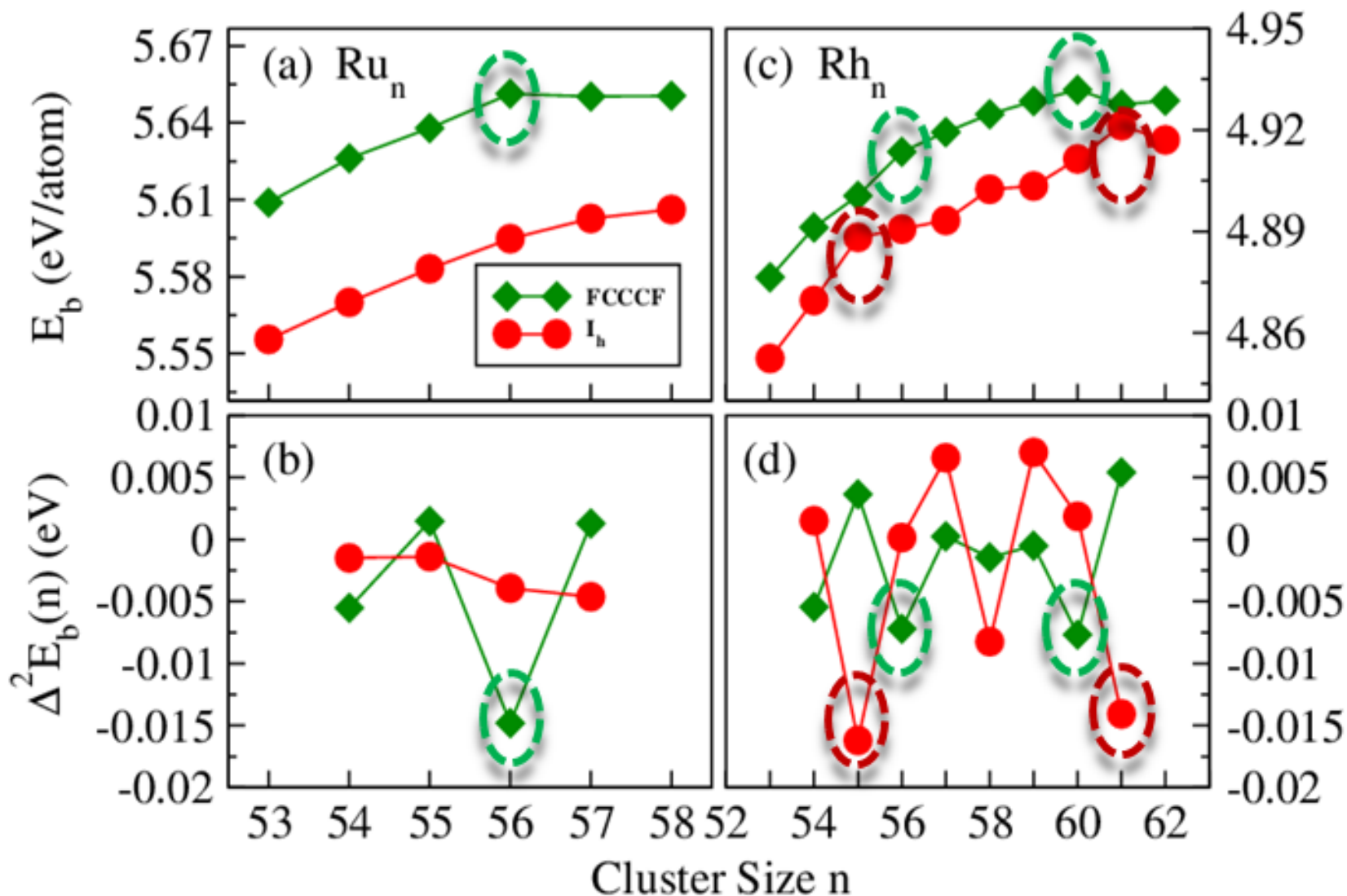


# What about other $TM_{55}$ ?



Almost all the  $4d$  and  $5d$ - $TM_{55}$  are non-icosahedron!

# What is (are) the real magic number(s)?



The edge energy shifts the well-known magic number 55 to even numbers

# Outline

- An Overview on Metals
- Why clusters?
- Discovery of magic metal clusters
- Competing formation mechanisms of magic clusters

# Major Competing Mechanisms for Formation of Magic Clusters

- Shells (especially for simple metals with delocalized electrons)
  - Electronic shells
  - Atomic shells
- Relativistic effects
- Wulff constructions
- Edge effects (generalized Wulff constructions)

# Case Study

- Calculation the work function of Diamond (111) surface: Geometry optimization of unit cell, cleave the (111) surface, build the supercell and geometry optimization, calculating the electrostatic potential energy profile
- Calculation the work function of Diamond (111) surface terminated by H

